R.A.M.S. ALANI

COMPARISON OF HYDROLOGIC AND HYDRAULIC FLOOD ROUTING, A CASE STUDY ON THE TIGRIS RIVER

THE GRADUATE SCHOOL OF NATURAL AND APPLIED SCIENCES
OF
ATILIM UNIVERSITY

RUAA ADNAN MOHAMMED SAEED ALANI

A MASTER OF SCIENCE THESIS
IN
THE DEPARTMENT OF CIVIL ENGINEERING

JANUARY 2020

ATILIM UNIVERSITY

COMPARISON OF HYDROLOGIC AND HYDRAULIC FLOOD ROUTING, A CASE STUDY ON THE TIGRIS RIVER

A THESIS SUBMITTED TO
THE GRADUATE SCHOOL OF NATURAL AND APPLIED SCIENCES
OF
ATILIM UNIVERSITY

BY

RUAA ADNAN MOHAMMED SAEED ALANI

IN PARTIAL FULFILLMENT OF THE REQUIREMENTS
FOR
THE DEGREE OF MASTER OF SCIENCE
IN
THE DEPARTMENT OF CIVIL ENGINEERING

JANUARY 2020

Approval of the Graduate School of Natural and Applied Sciences, Atilim University.

_____

Prof. Dr. Ali Kara
Director

I certify that this thesis satisfies all the requirements as a thesis for the degree of **Master of Science in Civil Engineering, Atilim University**.

_____

Prof. Dr. Mustafa Tokyay
Head of Department

This is to certify that we have read the thesis COMPARISON OF HYDROLOGIC AND HYDRAULIC FLOOD ROUTING, A CASE STUDY ON THE TIGRIS RIVER submitted by RUAA ADNAN MOHAMMED SAEED ALANI and that in our opinion it is fully adequate, in scope and quality, as a thesis for the degree of Master of Science.

_____	_____
Assist. Prof. Dr. Ibtisam Raheem Karim Co-Supervisor	Assist. Prof. Dr. Meriç Yılmaz Supervisor

Examining Committee Members:

Assoc. Prof. Dr. Yakup Darama
Civil Engineering Department, Atilim University _____

Assist. Prof. Dr. Meriç Yılmaz
Civil Engineering Department, Atilim University _____

Assist. Prof. Dr. Aslı Numanoğlu Genç
Civil Engineering Department, TED University _____

Date: *23 January 2020*

I hereby declare that all information in this document has been obtained and presented in accordance with academic rules and ethical conduct. I also declare that, as required by these rules and conduct, I have fully cited and referenced all material and results that are not original to this work.

Name, Last Name : RUAA ADNAN MOHAMMED SAEED ALANI

Signature :

ABSTRACT

COMPARISON OF HYDROLOGIC AND HYDRAULIC FLOOD ROUTING, A CASE STUDY ON THE TIGRIS RIVER

Alani, Ruaa Adnan Mohammed Saeed

M.Sc., Department of Civil Engineering

Supervisor: Assist. Prof. Dr. Meriç Yılmaz

Co-Supervisor: Assist. Prof. Dr. Ibtisam Raheem Karim

January 2020, 71 pages

This study deals with channel flood routing problem with two approaches: hydrologic and hydraulic flood routing using software programs HEC-HMS and HEC-RAS, respectively. For the comparison of these methods and software, a case study is carried out on a 158 km long reach on the Tigris River, between Al Shargat and Samarra Dam. With the observed inflow hydrograph of the flood event in the spring of 2019 as an input to both software, the routed outflow hydrograph is predicted. The peak discharge of the observed, HEC-HMS, and HEC-RAS outflows are obtained as 6437.00 m^3/s, 6538.70 m^3/s, and 6600.29 m^3/s, respectively. The translation of the HEC-HMS and HEC-RAS outflow hydrographs are estimated exactly the same as the observed outflow. The differences in the observed and estimated peak discharges are related with the lack of detailed data in HEC-HMS and added levees in HEC-RAS to prevent overflowing to floodplain in the study area. The observed and estimated outflow are found to be in good linear relation considering their coefficient of determination values close to 1.

Keywords: Hydrologic Flood Routing, Hydraulic Flood Routing, HEC-HMS, HEC-RAS, the Tigris River.

ÖZ

HİDROLOJİK VE HİDROLİK TAŞKIN ÖTELEMESİNİN KARŞILAŞTIRILMASI, DİCLE NEHRİ ÜZERİNDE ÖRNEK ÇALIŞMA

Alani, Ruaa Adnan Mohammed Saeed
Yüksek Lisans, İnşaat Mühendisliği Bölümü
Tez Yöneticisi: Dr. Öğr. Üyesi Meriç Yılmaz
Ortak Tez Yöneticisi: Dr. Öğr. Üyesi Ibtisam Raheem Karim

Ocak 2020, 71 sayfa

Bu çalışma, nehir taşkın öteleme problemini iki yaklaşımla ele almaktadır: sırasıyla HEC-HMS ve HEC-RAS yazılım programlarını kullanarak hidrolojik ve hidrolik taşkın öteleme yöntemleri. Bu yöntem ve yazılımların karşılaştırılması için, Dicle Nehri üzerinde Al Shargat ve Samarra Barajı arasındaki 158 km'lik kısımda bir örnek çalışma yapılmıştır. Her iki yazılıma girdi olarak 2019 ilkbaharındaki sel olayının gözlemlenen giriş hidrografı verilerek, ötelenmiş çıkış hidrografı tahmin edilmiştir. Gözlenen HEC-HMS ve HEC-RAS çıkış akımlarının pik debileri sırasıyla 6437.00 m^3/s, 6538.70 m^3/s ve 6600.29 m^3/s olarak elde edilmiştir. HEC-HMS ve HEC-RAS çıkış pik debilerinin zamansal ötelenmesi, gözlemlenen çıkıştakiyle tamamen aynıdır. Gözlenen ve tahmin edilen pik debilerdeki farklılıklar HEC-HMS'te ayrıntılı veri eksikliği ile HEC-RAS'ta ise çalışma alanında taşkın yatağına su basmasını önlemek için seddeler eklenmesiyle ilişkilidir. Determinasyon katsayılarının 1'e yakın olduğu göz önünde bulundurularak gözlenen ve tahmin edilen çıkış akımlarının iyi bir doğrusal ilişki içinde olduğu saptanmıştır.

Anahtar Kelimeler: HidrolojikTaşkın Öteleme, Hidrolik Taşkın Öteleme,HEC-HMS, HEC-RAS, Dicle Nehri.

To my super Mother who believed in my intelligence from childhood,

Who stay awake all nights during my exams

Who pray for me and my success

Who push me forward when everyone leaves me alone

To my father's soul

To my great supervisor (Dr. Meriç Yılmaz)

To my awesome co-supervisor (Dr. Ibtisam R. Karim) who support me

From bachelor days till now, and in PhD if God wills

To my beloved friends who encourage me in each step

I dedicate this effort

ACKNOWLEDGMENTS

I would like to express my thanks to all professors in Civil Engineering Department in Atılım University.

I shall also thank my co-supervisor in Iraq, Assist. Prof. Dr. Ibtisam R. Karim. Many thanks to both Moayad M. Ismail, and Dr. Ali Sadiq in the Civil Engineering Department in University of Technology in Iraq. Special thanks to Iraqi Ministry of Water Resources for providing the required data for this thesis.

Furthermore, I thank the members of the examining committee which represented by Assoc. Prof. Dr. Yakup Darama, Assist. Prof. Dr. Aslı Numanoğlu Genç, and my supervisor Assist. Prof. Dr. Meriç Yılmaz.

TABLE OF CONTENTS

LIST OF TABLES

TABLES

LIST OF FIGURES

FIGURES

CHAPTER 1

INTRODUCTION

1.1. General

A flood is a natural phenomenon that acts on human lives and economical losses. Floods may happen due to exceedance in the volume of water accessing the channel of river within a small time period, intending to spread in downstream direction especially in spring season due to excessive rainfall or ice melting.

Flood routing is a procedure to determine the flood hydrograph variation as water moves towards downstream through a channel (river) or a reservoir, named as channel routing or reservoir routing, respectively. Focusing on channel routing; it is a mathematical way of determining the change of the magnitude, velocity, and shape of the flood wave progressing on a channel reach over time. Flood routing may be classified as hydrologic or hydraulic, based on the solution of relevant equations [1]. Whichever the method is used, flood routing studies are of great importance for the prediction of flood effects on the downstream and flood protection studies.

1.1.1. Hydrologic Routing Methods

Hydrologic routing methods provide incredible computational proficiency and speed, requiring less detailed field information that customarily necessary for flood routing. The theoretical background of hydrologic routing methods is provided in Chapter 3 in detail. Here, hydrologic routing is described especially focusing on the limitations and difficulties.

The Muskingum routing strategy, which will be discussed in Chapter 3, has a few limitations which may influence the accuracy of the results obtained. Firstly, a prediction of Muskingum parameter K, storage constant (travel time of the flood

wave), is needed, which assumed to be remaining constant throughout the stream. This presumption is helpful and may deliver sufficient outcomes for several cases where the K parameter is subject to negligible variations. However, modeling flood routing with this assumption may be challenging, as the travel time of the flood wave is obviously varying with flow and channel characteristics. Secondly, the method gives a single stage-flow relation. In other words, for any given discharge, Q, there can only be one stage height. In fact, various stages could result for a known discharge as the geometry is not fixed along the channel. Moreover, the routing method is not adequate for steep hydrographs, flood of dams and bridges since its backwater impacts because of downstream shrinkage, huge inflow of tributary, or tidal diversity [2].

On the other hand, there are number of restrictions connected with this methodology. First, the hydrologic routing models performs expensive solutions, since experimental relations are applied to predict momentum effects. Thus, massive efforts and time could be utilized in calibrating these types of models with respect to historical data, and they may not be valid when applied to extreme events. The second difficulty associated with this method is that it requests a steady flow hydraulic analysis to convert the peak flow forecast into a stage. This analysis must either be done in advance for a number of potential flow scenarios, or be done on real-time basis for the specific forecast of peak flow [3].

1.1.2. Hydraulic Routing Methods

The theoretical background of hydraulic routing methods is also provided in Chapter 3 in detail. This part especially focuses on the advantages and difficulties of this method.

As the hydrologic routing method employs the rules of continuity equation and a single stage-discharge relation, the hydraulic routing method utilizes the full Saint-Venant equations, which compose of both the continuity and momentum equations. In this case hydraulic routing can give more precise results by considering the impacts of channel storage and wave shape [4]. For the hydraulic flood routing, a

few necessary assumptions are adapted like, the liquid is incompressible, which implies its density is constant, channel bed is stable, neglecting the vertical change in velocities, so that the vertical weight conveyance is hydrostatic [5].

Contrast to hydrologic flood routing strategies, the hydraulic flood routing strategy can calculate not only the flow depth, but also the streamflow rate with respect to time at each cross-sectional area provided in the model. In expansion, hydraulic routing methods can perform various conditions like breach of dams and tidal impacts.

Previous researches confirmed the practical application of hydraulic flood routing models, although it is expensive to get data of cross-sections along maybe hundreds of kilometers that affected by flooding, it provides accurate flood routing results can throughout a channel reach considered.

Although the fact that the hydraulic modeling integrates both the flood routing and water level forecasting into one step and provide accurate results with less calibration efforts, few agencies of flood forecasting are applying this approach. This can easily be clarified by the fact that most practitioners have deem to spend time and money in data collection and calibrating data for their available hydrological models, and there is no enough financial and human resources to learn and perform new models, unless it can be proved that there will be a significant privileges in terms of both time and accuracy. Given that the hydraulic models of unsteady flow, have a commonly reputation state that it is difficult to learn and implement, it became obvious that the forecasters are not confident about the value of utilizing hydraulic models operationally [3].

1.2. Aim and Scope of the Thesis

Salah Al Din is one of the important provinces in middle Iraq, that located near the Tigris River, with a population of about 1.6 million, faced frequent flood disasters during last years that caused both loss of lives and huge economic losses. Considering the lack of flood routing studies on this area, the aim of this study is to

find out the hydrologically and hydraulically routed outflow hydrograph at a downstream location, the velocity of the flood wave, the time, and the maximum water depth caused by the storm of flood wave over a reach on the Tigris River.

Among several software programs that could be used for hydrologic and hydraulic routing studies depending on the available information and required output, in this study HEC-HMS (Hydrologic Engineering Center - Hydrologic Modeling System) and one-dimensional HEC-RAS (River Analysis System) software programs developed by US Army Corps of Engineers Hydrologic Engineering Center are used, respectively. HEC-HMS is lumped and/or semi-distributed hydrologic model, where this distinction is based on the input data. HEC-RAS is a one-dimensional hydraulic model designed to help hydraulic engineers in channel stream examination and floodplain design. The output of the model can be applied in management of floodplain studies. Results of two software are obtained and compared to identify the suitable flood routing methods considering accuracy, data need, time and effort manners.

1.3. Thesis Description

This thesis is composed of five chapters. Contents of the chapters are as follows:

- An introduction to the thesis is made with the problem statement and the aim and objectives of the study are highlighted in Chapter 1.
- In Chapter 2, previous studies on flood routing in the literature are summarized.
- Methodology of the study is explained and the software programs HEC-HMS and HEC-RAS are introduced in Chapter 3. Governing equations of hydrologic and hydraulic flood routing are also presented in this chapter.
- The case study is described in Chapter 4. Results of the analyses and discussion of the results are also given in this chapter.
- In Chapter 5, conclusions of the study are presented. Also, several recommendations for future works are made.
- The cross-sections of the study reach in HEC-RAS software are presented in Appendix A.

CHAPTER 2

LITERATURE REVIEW

Hydrologic and hydraulic flood routing have always been of interest to researchers. As long as there are rivers and flood danger, flood routing will remain as a current issue. To enlighten the current and future studies, it is beneficial to overview the previous studies on flood routing.

2.1. Previous Studies on Hydrologic Flood Routing

Karim [1] used hydrologic and hydraulic flood routing methods on another reach of the Tigris River. For the hydrologic routing, Muskingum method for a nonlinear form and Muskingum-Cunge (linear and nonlinear form) have been applied, while the four-point implicit finite difference scheme was discussed to express the hydraulic routing, comparison between the mentioned method was applied to find out the hydraulic method as the most accurate one but more time and effort consuming.

Fung [6] applied three techniques of flood routing (Muskingum, Lag, and Storage routing), focusing on large–scale model. Sacramento Basin WARMF and HEC-RAS models have been utilized for hydrological data input as well as comparison. The results showed all models were applicable for flood routing but Muskingum method was the most accurate one.

Kumar et al. [7] examined the applicability of Muskingum method for flood routing, on Hirakud reservoir which is a part of Mahanadi River in India as a case study. Comparison has been conducted between two cases; one was controlled inflow from power station while the other was uncontrolled from tributary. Muskingum model has been improved for multi-sources inflow to figure out a single outflow for the

reach, suitable coefficient has been derived for each case, and the decision made for the Hirakud River gates was to open them once each 12 hours during the flood.

Barat et al. [8] investigated Muskingum-Cunge flood routing model for a reach of Karun River, Iran, as most of river basin were unmanaged due to the high cost of gauging station works. The field applications of Muskingum–Cunge flood routing model has been investigated using available daily and hourly flood data, in terms of the attenuation of the peak outflow, the lag of the peak outflow, and the volume. The results have been compared with other solutions i.e. dynamic and kinematic wave models) and others. The results showed the difference between Muskingum-Cunge and other benchmark methods became less when using smaller Manning roughness coefficient and bed slope.

Mohammed [9] computed the coefficients, for two hydrological flood routing methods, i.e. Muskingum and Muskingum-Cunge methods, on a reach from Shatt- Al Hilla in Iraq. The Muskingum routing coefficients, i.e. C_0, C_1, C_2 have been considered as constant values for Muskingum method, while the coefficients have various values for Muskingum-Cunge method, same as the number of sub-reaches, in addition to the condition of $C_1+C_2+C_3=1$ that has been achieved by both mentioned methods. The details of these coefficients are discussed in detail in Chapter 3.

Twumasi et al. [10] suggested that the basic relationships between rainfall and runoff should be understood since it is an important step in efficient control of flood water. High intensity short period rainfall causes flash floods in the driest area of Ghana, which is one of the disadvantageous properties of the arid and semi-arid areas. They used Geographic Information Systems (GIS) for catchment delineation and HEC-HMS for flood volume calculation. It has been concluded that both of hydrologic routing model and GIS mechanism can be used for computation of flood magnitude utilizing exact values of temperature, rainfall, and flow.

Haque et al. [11] studied North-East of Bangladesh where exposed to frequent flash flood. Due to flash floods on 2004, 2010, and 2016, there had been huge losses in

farm areas. An essential step to reduce such kind of losses is developing an early warning system for flood prone regions. A hydrological model has been established using HEC-HMS for Meghan River basin with 7000 km^2 drainage area and discharge at Sunamganj station has been simulated. SCS (Soil Conservation Service) Curve Number method has been used to estimate runoff volume. HEC-HMS model accomplishment has found to be satisfactory and this model might be considered as valuable tool for flash flood prediction for future.

Sinha et al. [12] considered Sone River bank in India as a case study. Muskingum method has been applied to estimate the inflow and outflow, graphical method and least square method has been utilized in order to calculate the parameters of Muskingum method. The results of the two mentioned methods have been compared. The results will be used in flood protection purposes. Exact information like the flood peak has been recognized as most significant parameter affecting the flood protection works.

2.2. Previous Studies on Hydraulic Flood Routing

McKay [13] developed a model for hydraulic flood routing, as the data collection for hydrologic modeling is so expensive and not always available. The importance of flood forecasting especially for people living around the river bank was highlighted and minimum necessary data has been specified in order to use in flood routing model.

Hicks and Peacock [3] used HEC-RAS model, which is usually utilized for steady flow hydraulic routing, to analyze unsteady flood routing. Peace River in Alberta has been taken as case study and with the use of significant data of a flood in 1987, the capability of HEC-RAS for unsteady flood forecasting has been examined, and accurate results have been achieved compared to other hydrologic routing models like SSARR (Streamflow Synthesis and Reservoir Regulation System) model.

Sun [5] developed a HEC-HMS model for the Soap Greek watershed. Muskingum routing method has been employed in this model, in order to simulate the impacts of

the existing flood protection practices on peak discharge. HEC-RAS model has also been adapted for the case study area. Comparison between the results of hydrologic and hydraulic method been conducted to clarify that HEC-RAS simulates the flood hydrograph more accurate than HEC-HMS.

Havel [14] examined the effects of wildfires of High Park and Hewlett that occurred in USA, Colorado in 2012. Two well-known hydraulic models have been utilized; the results of Soil and Water Assessment Tool (SWAT), used in modeling the hydrology of the upper Cache la Poudre basin, have been used as input for HEC-RAS, in order to simulate stream flows. The results found to be satisfactory for simulating after-wildfire conditions in the area.

Mai and De Smedt [15], applied HEC-RAS model has been applied to simulate flood flow and predict water profile precisely at the downstream of Hong River basin in combination with the use of a hydrologic model (Wet Spa) for flood simulation within the mountainous upper sub-basin. The combined model found to be valuable in creating flood forecasting and early warning studies to lessen the losses due to flood evets in Vietnam.

Husain [16], used HEC-RAS considering on three components of one-dimensional hydraulic analysis; water surface profile calculation, simulation of unsteady flow, and sediment transport. He concluded that the major aim of hydraulic modeling is to supply a system to manage flood control, and the capability of HEC-RAS in simulation of water surface profile at different locations of reach of study has been proved. In addition, the output of HEC-RAS has been used in computing the bridge overtopping in reach of study.

Shayannejad et al. [17] focused on an example of unsteady flow that has been solved by using HEC-RAS as the solution of Saint-Venant equation is so complicated. The methodology of research has been used for tree-type and looped channel networks, to obtain numerous critical depths in the study reach. The incident of just one critical

depth in involved cross section with developed geometry was shown for the tree-type channel network.

It became obvious that, there are variety of methodologies of both hydrological and hydraulic flood routing which are successfully applied on different case studies. All these models generally characterize the time variation of hydrodynamic channel variables like stage and velocity to estimate outflow at downstream in order to predict shape and magnitude of flow wave which might be used in flood forecasting to minimize both life and economic losses.

CHAPTER 3

THEORETICAL BACKGROUND

Flood routing is a mathematical procedure for estimating the magnitude, velocity, and shape of a flood wave with respect to time (i.e., the flow hydrograph), at one or various points along a channel. Flood routing can be classified as a hydrologic or hydraulic routing method; routing by a lumped system method is called hydrologic routing, while routing by a distributed system method is called hydraulic routing [18]. This chapter provides detailed descriptions of the hydrologic and hydraulic routing methods.

3.1. Hydrologic Flood Routing

Hydrologic flood routing basically utilizes confined physical parameters of the channel, as it mathematically depends on continuity equation, and on the other hand the relation between the water storage and the discharge at outlet.

3.1.1. Theoretical Analysis of Hydrologic Flood Routing

3.1.1.1. Continuity Equation

The mathematical statement in fluid mechanics mentioned that, for a fluid passing through an open channel in a steady flow, the mass of fluid flowing through any section of the channel in a unit of time is constant as in Figure 3.1. The continuity equation represents the change in velocity in a way that:

$$A_1V_1 = A_2V_2 \quad \text{(3.1)}$$

Here, A is the cross-sectional area and V is the velocity of fluid (water).

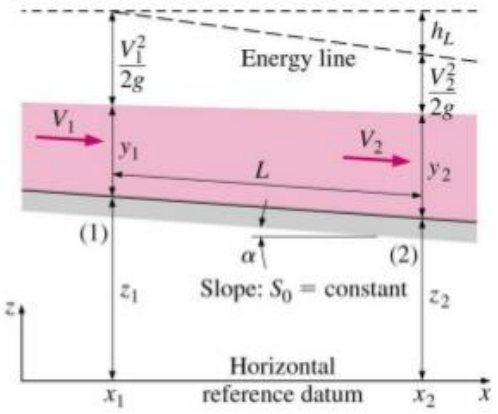

Figure 3.1 Flowrate volume for unsteady flow in open channels [19]

3.1.1.2. Storage Concept

The relation between the upstream and downstream where outflow could be measured indicates the change in stored water volume which is known as storage, i.e. the difference between inflow and outflow is equal to the rate of change in storage in the channel with respect to time [20].

$$\bar{I} - \bar{Q} = \Delta S / \Delta t \quad \text{..... (3.2)}$$

Here, $\bar{I}$ is the average inflow to the reach, $\bar{Q}$ is the average outflow from the reach, ΔS is the change of storage, and Δt is the time increment.

Equation (3.2) indicates that the storage of the channel reach is a function of I and Q, or,

$$S = f(I, Q) \text{ .....} \quad \text{..... (3.3)}$$

Here, S is the storage in the channel reach.

3.1.2. Hydrologic Flood Routing Methods

3.1.2.1. Muskingum Method

The Muskingum hydrologic routing method models the storage volume of flooding in a channel as the sum of wedge and prism storage, as shown in Figure 3.2. The storage under the steady-flow water surface profile that called prism storage, while wedge storage is the further storage below the actual water surface profile. This method was developed for the design of flood protection system of the Muskingum River basin [21].

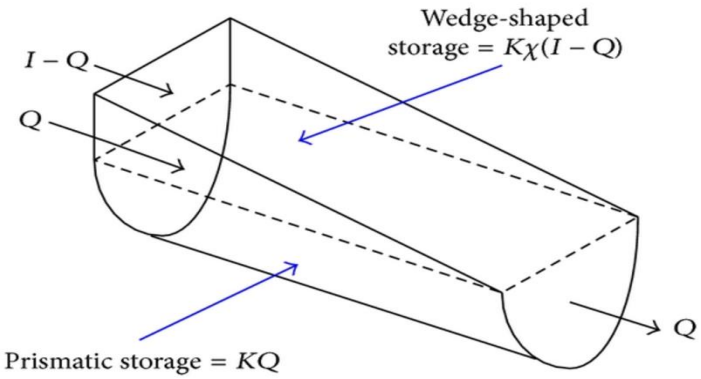

Figure 3.2 Prism and wedge storages [1]

The volume of prism storage, S_{Prism} is:

$$S_{prism} = K\,Q \quad \text{..... (3.4)}$$

And the volume of wedge storage, S_{Wedge} is:

$$S_{wedge} = K\ X\ (I - Q) \quad \text{..... (3.5)}$$

Where, K is the storage constant or approximately the travel time of the flood wave through the reach, and X is the dimensionless weight factor between inflow and outflow.

By summation of the Equations (3.4) and (3.5), the basic Muskingum equation is obtained as:

$$S = K * [X * I^m + (1 - X) * Q^m] \quad \text{.....} \quad (3.6)$$

Where, m is the power to express the nonlinear relation between storage and discharge. For simplicity and practical purpose, m in the above mentioned equation is assumed to be unity, Thus, the working Equation (3.6) has been developed to take the form in equation (3.7).

$$S = K * [X * I + (1 - X) * Q] \quad \text{.....} \quad (3.7)$$

This equation expresses the linear relationship of storage to inflow and outflow. The weighting factor, X is having a range of $0 \leq X \leq 0.5$, depending on the shape of the wedge storage. It is zero for reservoir type storage (zero wedge storage or level pool case S = KQ) and 0.5 for a full wedge. In natural streams mean value of X is near 0.2. The parameter K is the time of travel of the flood wave through the channel reaches also known as storage time constant and has the dimensions of time [20] **.**

According to Linsley et al. [22], to find the coefficients of linear Muskingum method, various values of X must be assumed and then, observed values of inflow and outflow must be used to draw the values of cumulative storage S on the vertical axis versus values of [X*I+ (1-X)*Q] for a given X value on the horizontal axis. The resulting shape will be like a loop as shown in Figure 3.3. Repeating this process for different values of X, the value of X which the loop most resembling a straight line must be chosen. The slope of this straight line will be represented by the K parameter.

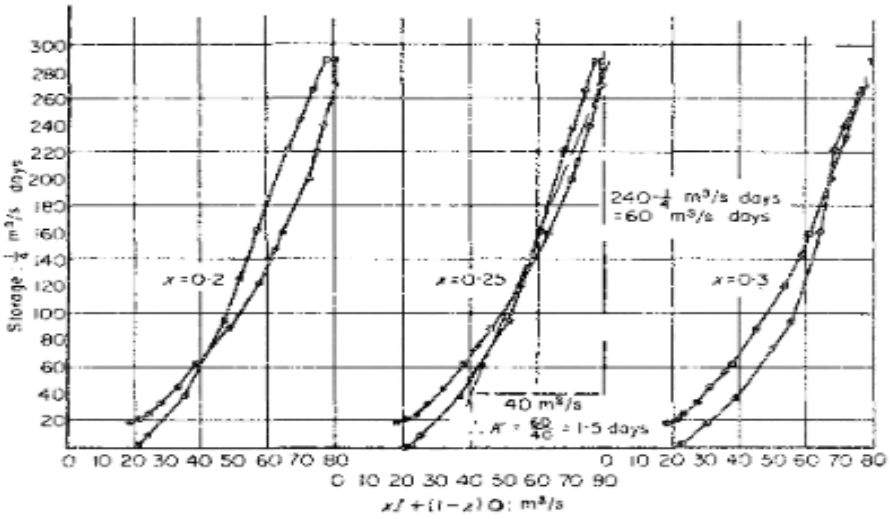

Figure 3.3 Loop relation in parameters estimation [23]

Substituting Equation (3.7) in the Equation (3.2) yields the routing equation for the Muskingum method as [21]:

$$Q_2 = C_0 I_2 + C_1 I_1 + C_2 Q_1 \quad \text{..... (3.8)}$$

The three coefficient C_0, C_1, C_2 calculated as:

$$C_0 = \frac{\Delta t - 2KX}{2K(1-X) + \Delta t} \quad \text{..... (3.9a)}$$

$$C_1 = \frac{\Delta t + 2KX}{2K(1-X) + \Delta t} \quad \text{..... (3.9b)}$$

$$C_2 = \frac{2K(1-X) - \Delta t}{2K(1-X) + \Delta t} \quad \text{..... (3.9c)}$$

Here, C_0, C_1, and C_2 are Muskingum routing coefficients and are functions of the parameters K and X. Summation of three coefficients must be unity:

$$C_0 + C_1 + C_2 = 1 \quad \text{..... (3.10)}$$

3.1.2.2. Muskingum-Cunge Method

Cunge [24] advanced the use of the Muskingum method by explaining how the parameters K and X could be related to the hydraulic properties of a simplified, prismatic channel. These are based on linking the convection diffusion model to the Muskingum routing equation. The parameters of the traditional Muskingum method can only be determined from stream gage data. This makes the Muskingum-Cunge method more favorably applied to ungaged streams. The equations for K and X in the Muskingum-Cunge method are [24]:

$$X = \frac{1}{2}\left(1 - \frac{Q}{BS_0 c\Delta x}\right) \quad \text{(3.11)}$$

$$K = \frac{\Delta x}{c} \quad \text{(3.12)}$$

Here, B is the bottom width or average width of the channel, S_0 is the channel bottom slope, c is the flood wave celerity, and Δx is the distance increment. Those equations above lead to the determination of outflow discharge as follows:

$$Q_{i+1}^{j+1} = C_1 Q_i^{j+1} + C_2 Q_i^j + C_3 Q_{i+1}^j \quad \text{(3.13)}$$

3.1.3. Hydrologic Flood Routing Modeling with HEC-HMS

3.1.3.1. HEC-HMS Background

Hydrological models are founded on a group of connected equations that switch the physical rules, which are quite complicated natural phenomena, to kind of mathematical shape. The main challenge that faced by the hydrological models is the lack of availability and high cost of hydrologic data [11]. Various models can be applied, depending on the conceived output, the available database, input variables, analysis, and degree of accuracy required.

HEC-HMS is a public flood routing modeling tool developed by the Hydrologic Engineering Center of the US Army Corps of Engineers, counted as a standard for hydrologic simulation in the USA [25]. The program which began as HEC-1, first version in 1992, has been improved into fully integrated graphical user interface. The second major emission of the model caused changes that made it possible to persistent model, with dry and wet periods. It is a numerical model that contains a huge set of techniques to simulate watershed, behavior of channel, and water-control structure, as well as predicting flow, timing, and stages. The HEC-HMS emulation manners act watershed precipitation, magnitude of runoff, runoff including base flow, interflow, and channel flow.

In this study HEC-HMS is used for hydrologic flood routing calculations; since HEC-HMS depends on these components [26]:

- Basin model, which describes the various factors of the hydrologic method subdivision, reaches, cross-sections, resources, and diversion.
- Meteorological model, that characterize the modeling both of heavy rain and evaporation process in spatial and temporal manner.
- Control specialization, in which defines the simulation time window.
- Time series data, actual time series data for all the meteorological factors defined in meteorological model are provided in this part. A portion from mentioned data, can be provided for simulation of the developed model. It can be supplied to the software both manually or by HEC-DSS (Hydrologic Engineering Center Data Storage System).
- Paired data, graphical form of meteorological data are provided as paired data.

The accomplished hydrographs by model can be utilized for studies of water availability, flow forecasting structure, design of reservoir spillway, floodplain arrangement, urban drainage, and systems operation with attached extra software Arc View GIS 3.2 [26].

The HEC-HMS model is lumped and semi-distributed model designed to simulate rainfall - runoff processes in a wide range of geographic areas, from wide river basin

water supplies and flood hydrology to small urban and natural watershed runoffs. It simply operates huge tasks in respect to hydrological studies, covering losses, runoff transform, analysis of meteorological data, open channel routing, rainfall-runoff simulation, and parameter estimation. However, the HEC-HMS utilizes separate models that calculate runoff volume, models of direct runoff, and models of base flow. It contains nine various loss methods, part of them are designed primarily for event-based simulation, while others are intended for continuous simulation [27].

Previous studies on HEC-HMS proved its capability to simulate and forecast stream flow depending on various datasets and catchment types [28]. A large portion of these studies obviously mentioned that the results of the model simulation are specific, in that different conjunctions of a model set containing the loss methods, runoff transform methods, and base flow separation mechanisms were found to respond variably [29].

There are five hydrologic routing methods available for the HEC-HMS model: the Kinematic Wave Routing, Lag Routing, Modified Puls Routing, Muskingum Routing, and Muskingum-Cunge Routing methods; the Muskingum method is selected for the present study because it is commonly used and can provide reasonably accurate results for moderate to slow rising floods propagating through mild to steep sloping watercourses [18].

3.1.3.2. HEC-HMS Overview, Methodology, and Input and Output

Together with the runoff simulation, HEC-HMS provides the following outputs [18]:

- Events that present the upper limit of precipitation possible at given location
- Estimate the volume of runoff by loss model.
- Direct runoff model that can account overland flow, storage, energy losses.
- Hydrologic routing model that account for storage as water move through channel.
- Water control measures model.
- An automatic calibration package.

A conceptual log frame serves to describe the overall study procedure. The essential data kinds are requested as input contains rainfall, DEM (Digital Elevation Model), soil and land use data, and meteorological data for model. After data input step, HEC-HMS models are run. The major output from model is outflow at the outlet of the catchment. Finally, the output is compared with the observed discharge at selected gauging of the basin [27]. The HEC-HMS methodology flow diagram is provided on Figure 3.3.

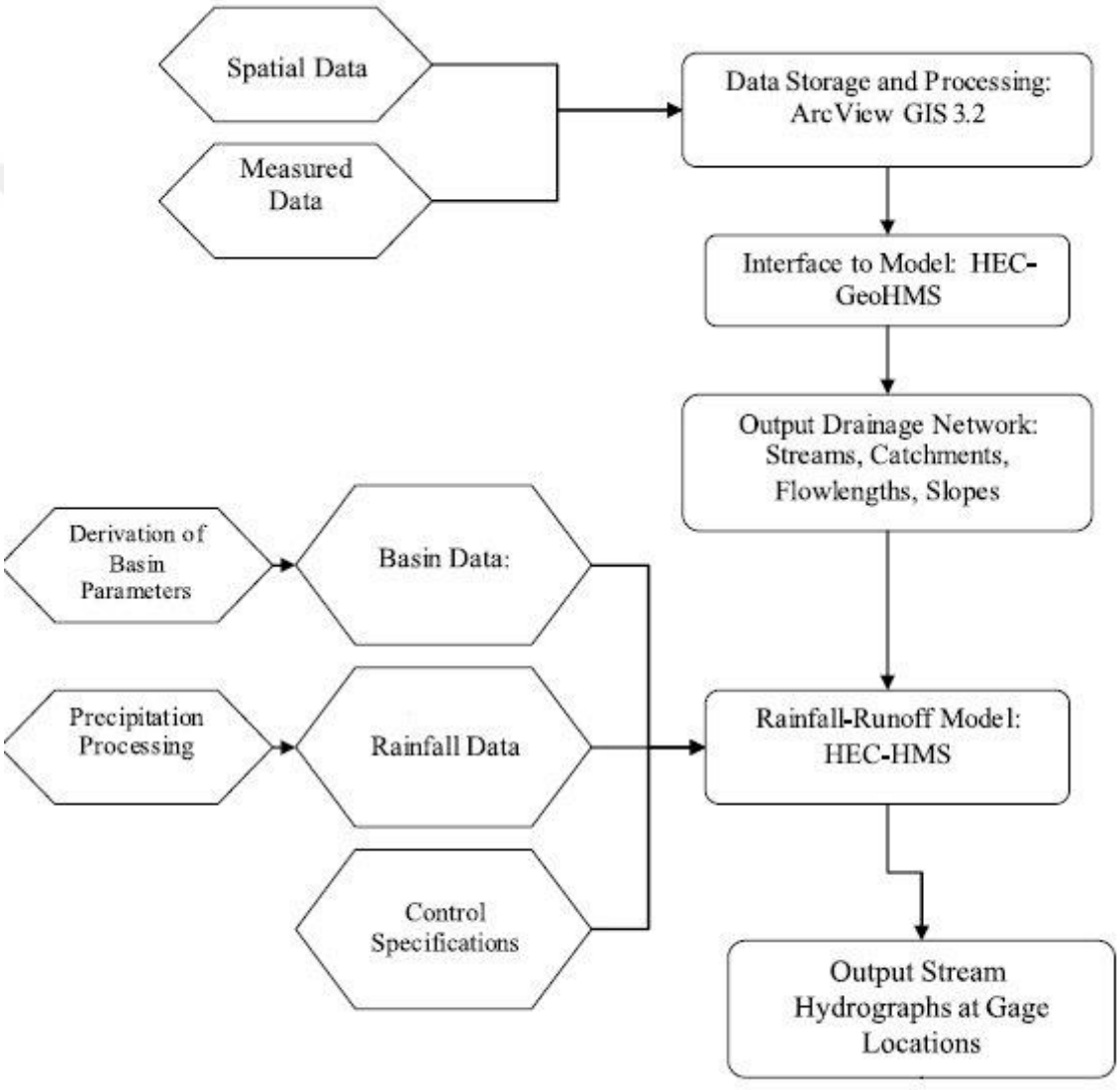

Figure 3.4 HEC-HMS methodology flow diagram [30]

3.2. Hydraulic Flood Routing

Hydraulic flood routing techniques supply a practical alternative to hydrologic flood routing; they are basically depending on conservation of both mass and longitudinal momentum; so they need detailed data describing both the topographic and hydraulic features of the river reach that need to be modeled. Their greatest restriction is the high cost required to get survey data for long study reaches.

Solution of conservation of mass and momentum equations are complex due to three-dimensional nature of the open channel flow. However, for practical purposes velocity of the flow is assumed to vary only along the longitudinal axis of the channel, i.e. one-dimensional flow is assumed. The well-known Saint-Venant equations can be applied in hydraulic flood routing studies to solve the unsteady open channel flow parameters. The assumptions made by these equations are [31]:

- Flow is one-dimensional.
- Hydrostatic pressure distributed on the flow of vertical surface.
- Manning's equation can be utilized, as the frictional strength is as same as in unsteady flow and for the corresponding depth in uniform flow.
- The bed slope is small and constant along the reach.

3.2.1. Theoretical Analysis of Hydraulic Flood Routing

3.2.1.1. Continuity Equation

As mentioned in the beginning of this chapter, the continuity equation is represented as in Equation (3.2). This equation is substantial for a prismatic or a non-prismatic channel; a prismatic channel is one in which the cross-sectional shape does not vary along the channel and the bed slope is constant.

3.2.1.2. Momentum Equation

The application of the momentum equation allows the hydraulic routing method to account for more physical characteristics, including the bed slope, the roughness,

geometry, and length of channel. Compared to hydrologic routing methods, the hydraulic routing method can compute not only the water depth but also the flow rate with respect to time at each cross section.

The momentum equation as an expression of Newton's second law of motion represents the transient force balance on the fluid within a slice of the channel cross-section; the rate of variation of stored momentum through the volume of control plus the momentum flux across the control surface is equal to the summation of applied forces. The applied forces acting on the element of fluid volume shown in Figure 3.5 is as follows [31]:

$$\Sigma F = F_g + F_f + F_e + F_p \quad \text{..……..……..} \quad (3.14)$$

Here, F_g is the gravity force, F_f is the friction force, F_e is the expansion energy losses, and F_p is the pressure force.

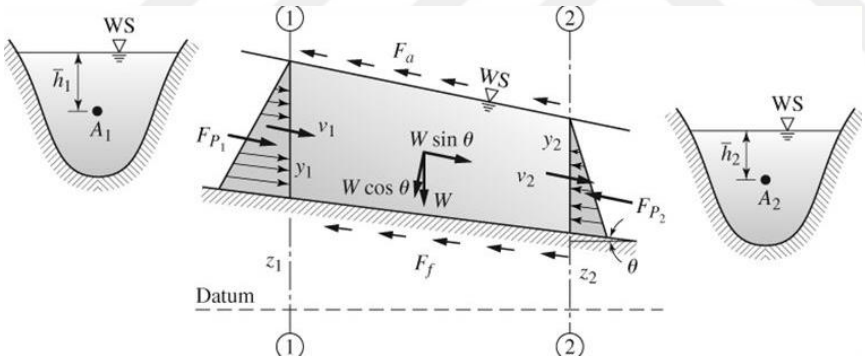

Figure 3.5 Acting forces of the water in channel reach [32]

- Gravity Force: For a small channel bed slope angle, θ, the channel bed slope S_0 is approximately equal to sin θ. Therefore, the simplified weight component acting in the downstream direction named as the gravity force is:

$$F_g = \rho g A S_0 dx \quad \text{……...……...……..} \quad (3.15)$$

Here, ρ is the density of water, g is the gravitational acceleration, dx is the length increment in the flow direction.

- Friction Force: The friction force due to shear stress, τ, acting on the wetted parameter, P over the length, dx of the reach is:

$$F_f = -\tau P \mathrm{d}x \quad \text{(3.16)}$$

Since,

$$\tau = \rho g R \mathrm{S}_f \quad \text{(3.17)}$$

$$F_f = -\rho \mathrm{g} A S_\mathrm{f} \mathrm{d}x \quad \text{(3.18)}$$

Here, R is the hydraulic radius (R= A/P) and S_f is the friction slope.

- Expansion energy losses: Expansion of the channel that lead to energy loss within turbulent motion, acts as minor losses. The magnitude of eddy losses is connected to the alteration in velocity head through the length of channel proceeding the losses. These eddy losses are given by:

$$F_e = -\rho \mathrm{g} A S_\mathrm{e} \mathrm{d}x \quad \text{(3.19)}$$

Here, S_e is the eddy loss slope

- Pressure force: The pressure force on the vertical surface of flow is hydrostatic since the surface curve is small, (according to the Saint-Venant equation assumptions). The hydrostatic force on the left end, F_{pL} and right end, F_{pR} of the element in Figure 3.5 are:

$$F_{pL} = \rho g A \bar{h} \quad \text{(3.20)}$$

$$F_{pR} = \rho g A\bar{h} + \rho g A(\partial y/\partial x)dx \quad \text{..... (3.21)}$$

Here, $\bar{h}$ is the distance from water surface to the centroid of cross-section area. The unbalanced pressure force, F_p is the result of the difference of hydrostatic force on the left side, F_{pL} and the hydrostatic force on the right side F_{pR}:

$$F_{pR} = -\rho g A(\partial y/\partial x)dx \quad \text{..... (3.23)}$$

The summation of forces determined above gives the resultant force on the element:

$$\Sigma F = \rho g A S_0 dx - \rho g A S_f dx - \rho g A S_e dx - \rho g A(\partial y/\partial x)dx \quad \text{..... (3.24)}$$

The Saint-Venant equations, accounting for continuity and momentum equations, are the governing equations for one-dimensional, unsteady flow in an open channel as follows:

$$dv/dt + v\, dv/dx + g\, dy/dx + S_0 + S_f = 0 \quad \text{..... (3.25)}$$

3.2.2. Hydraulic Flood Routing Modeling with HEC-RAS

3.2.2.1. HEC-RAS Background

The Saint-Venant fundamental equations first presented in 1871, present a complete form of the governing forces of the flow. Solving these kind of equations, especially in open channels with irregular sections, needs a lot of computational efforts and time [19]. It is essential to use computer programs for the numerical solution of these equations. By using such models, profile of water levels can be plotted in each branch of the channel network at any time.

HEC-RAS is a one-dimensional steady flow hydraulic model designed to support hydraulic engineers in channel flow analysis and computing of floodplain; the results

obtained by the model can be utilize in both floodplain management and flood insurance researches [3]. HEC-RAS system includes variety of river analysis components for [25]:

- Steady flow water surface profile computations.
- One- and two-dimensional unsteady flow simulations.
- Movable boundary sediment transport computations.
- Water quality analysis.

All four components mentioned above, utilize a usual geometric data representation and common hydraulic computation routines. In addition to the river analysis components, the system includes detailed hydraulic computations as follows:

- Mixed flow regime analysis; allowing analysis of both subcritical and supercritical flow regimes in a single computer run.
- Bridge and culvert analysis and design, including FHWA culvert routines for elliptical, arch, and semi-circular culverts.
- Multiple bridge and culvert openings of different types and sizes at a roadway crossing.
- Bridge scours computations following FHWA Publication HEC-18.
- Bridge design editor and graphical cross section editor.
- Floodplain and floodway encroachment modelling
- Multiple profile computations.
- Lateral flow, split flow, over bank dendritic networks.
- Sediment Impact Analysis Methods (SIAM).
- Water quality capabilities (temperature modelling).
- Tidal boundary conditions.
- Reservoir and spillway analysis
- Levee overtopping.
- User defined rules for controlling gate operations.
- Flooded areas pumping
- Modeling for pressurized pipe flow.

CHAPTER 4

CASE STUDY, RESULTS, AND DISCUSSIONS

4.1. Study Area

The reach that has been taken for this study located in Salah Al din province, the center of it called Tikrit, at 190 km north of Baghdad that occupied 24,751 km^2 of area, making it the fifth largest province in Iraq, with a population of 1,595,000 [33]. Among its nine districts, Al Shargat which has a privileged geographical location that connected three provinces located at 115 km south of Nineveh, 125 km north of Tikrit, and 135 km west of Kirkuk. Tigris River passes through Al Shargat and separates into two parts; eastern and western. The economy of this area depends on agriculture especially wheat and barley.

Length of the reach is approximately 158 km on Tigris River bounded by Shargat station at upstream and the Samarra Dam station at downstream as in Figure 4.1. The Samarra Dam (see Figure 4.2) is located on Tigris River, west of Samarra, the well-known city according to its historical landmarks. The main purpose of construction of this dam is to transfer the water from Tigris River to the Tharthar Lake to control flood, provide sufficient quantities of water for irrigation to the implanted areas, and to generate hydroelectric power.

The Samarra Dam and the Tharthar Lake are parts of the Tharthar project. Due to the importance of this project, the Construction Council that was formed in 1950 tasked the Code Wilson international consulting company to prepare the required designs, specifications, and contract terms for the Tharthar project, in order to relief of flood risks from the city of Baghdad and secure water to irrigate extensive agricultural lands located between Samarra and Baghdad.

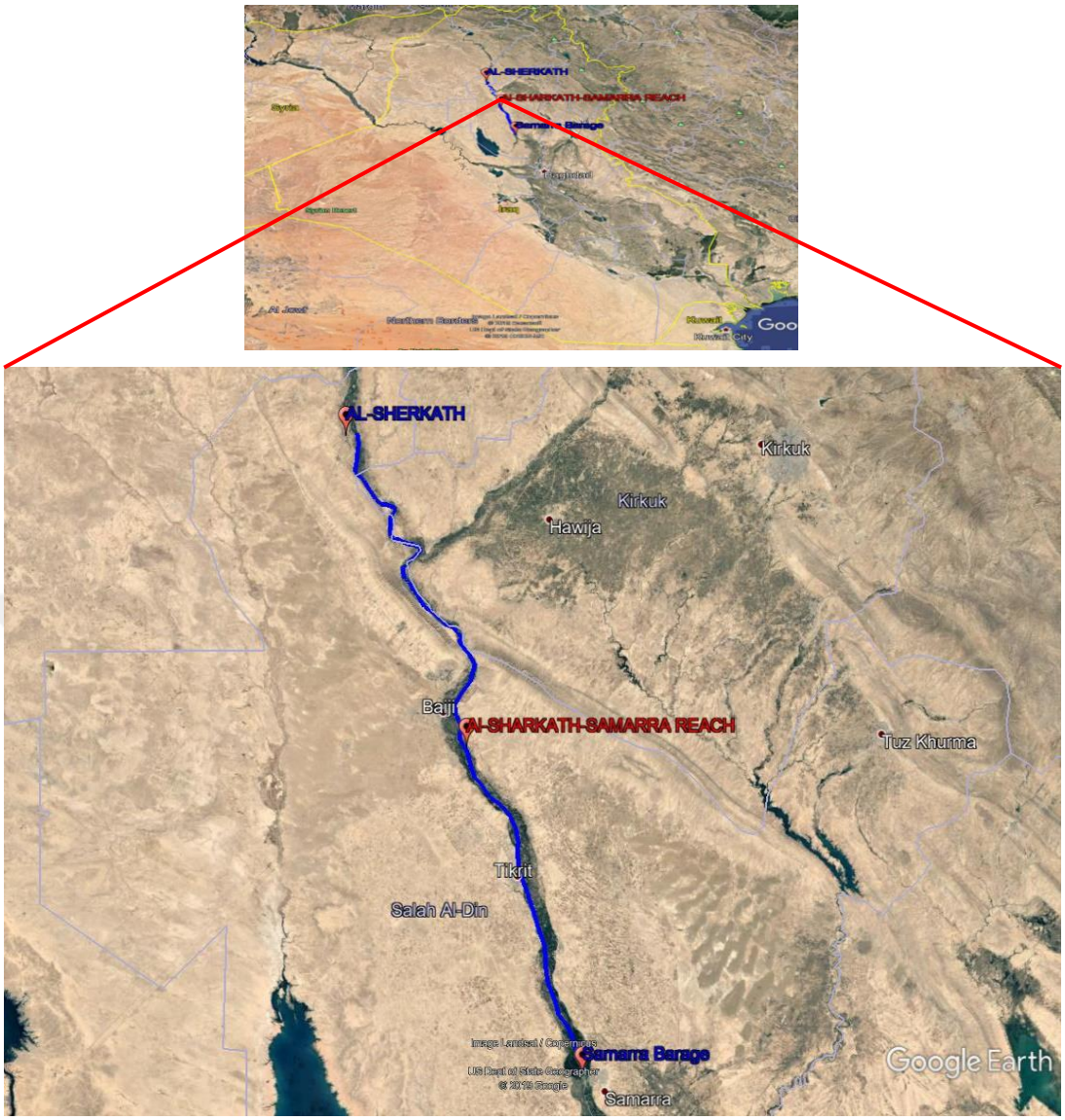

Figure 4.1 Reach of the River Tigris between Shargat and Samarra

In February 1952, the works of the Samarra Dam on the Tigris River and its related activities were transferred to the German company, Züblin that proposed the construction of the dam at the city of Samarra after the consultants' proposal was to be built in the north city. A secondary contract for the supply of gates and iron parts was also transferred to the English company, Ransem & Rapper.

The German company, Züblin has pledged to complete the work on 1 March 1956 so that the flood water for that year can be converted to the Tharthar Lake, and the water was actually diverted from the Tigris River to the Tharthar Lake on April and

May of 1956 as the rate of drainage passed in the channel leading to Tharthar was 836 m^3/s during April and 114 m^3/s during May.

Figure 4.2 The Samarra Dam

The main installations with the Samarra Dam include a regulator of the Tigris-Tharthar canal to drain the flood water into the Tharthar Lake. The Samarra Dam is located opposite of the city of Samarra, and it was established on the right side of the Tigris River, then the river water was diverted to dam to run through it after closing the main course of the river with soil plugs. There are 17 gates on the dam, each one with 12 m width, and 4.8 m height [33]. It is equipped with iron gates that move by electric force or by means of manually operated levers in case of electricity shortage.

The dam consists of a concrete structure with a length of 252 meters and a concrete bottom with 16 supports. The purpose of constructing the dam is to control the water of the Tigris River and raise the water surface elevation from 63 m to 69 m above the sea level, in order to convert the flood water to the Tharthar Lake.

At the dam site, there is a hydroelectric station, with 14 openings, the width of each hole is 10 m, 6 of them were exploited to construct the hydroelectric station, which is connected with the Samarra Dam to reach the length of the dam and the station to

449 m. The hydroelectric station was completed in 1971 and is composed of three turbines to generate 84 MW at maximum, and this station operates at lower level in the forefront as 67.3 m above sea level with a level not less than 55.7 m.

The level of the dam openings threshold is 58 m and the backside flood level is 52 m. The maximum discharge through the dam to the Tigris River is 7000 m^3/s and the maximum discharge diverted to the Thartar Lake is 9000 m^3/s [33]. The dam was not equipped with a water transport corridor, due to the lack of expectation of an active navigation movement on the Tigris River, in the north of the Samarra Dam.

This specific area faced flood threats within last years, as 1500 people dislocated from the villages on the banks of the Tigris in Biji on January 2013 due to flooding of the Tigris River as water surface increased by 4 m above the normal level, leading to destroy the floating bridge between Al Mishag and Al Ziwiya villages. This flood event forced the authorities to take relief actions such as opening gates of the Samarra Dam in order to discharge water to the Tharthar basin. On 23 November 2018 have led to loss of lives, 3000 houses sank, hundreds of cars damaged, large number of cattle death, and 1400 residents dislocated from many villages in Shargat as the Tigris River flooded due to heavy rain and lack of infrastructure, making the interior streams unable to discharge large quantity of water. The local authority announced emergency situation [34].

According to the Iraqi Ministry of Water Resources formal website, the Samarra Dam faced a huge flood wave due to heavy rainfall on 25 March 2019; as the discharge of the Samarra Dam exceeded 10000 m^3/s that led to 2 m increase in water surface level, as Dokan and Darbandikhan Dams already reached their max storage capacity since extra quantities of water contribute to the river from Greater Zab and Lesser Zab. The Samarra Dam capacity was not enough to absorb the flood wave, as Iraq has not faced that much heavy rain since long years. One of the suggested solution is to create a hole in the west side of dam in order to pump more quantities of water to the Tharthar Lake with storage capacity exceeding 120 billion m^3 which represents the strategic water storage in Iraq.

4.2. Part 1: Hydrologic Routing Studies

For the hydrologic routing studies, HEC-HMS needed main input like Muskingum parameters K and X, and hydrograph at upstream Shargat station. Then, the software would predict the hydrograph at downstream Samarra station. HEC-HMS treats the river as a single reach and no need to create many section, in contrast to HEC-RAS. Data that have been recorded at the observation stations which are presented in Table 4.1 and Figure 4.3, are obtained from Iraqi Ministry of Water Resources for the flood wave at March 2019 at every 12 hours.

Table 4.1 Observed inflow at Shargat station and outflow at Samarra station

Time	**Date**	**Inflow**	**Outflow**	**Ave. Inflow**	**Ave. Outflow**	**Storage**
hr		**(m^3/s)**	**(m^3/s)**	**(m^3/s)**	**(m^3/s)**	**(m^3)**
0	1 March	925.29	852.25			5000
12	1 March	1363.06	912.41	1144.18	882.33	83553
24	2 March	2069.46	1143.02	1716.26	1027.71	290118
36	2 March	3183.79	1594.21	2626.63	1368.61	667522
48	3 March	4397.61	2336.17	3790.70	1965.19	1215176
60	3 March	5432.34	3248.58	4914.98	2792.37	1851957
72	4 March	6268.09	4211.12	5850.22	3729.85	2488067
84	4 March	6745.66	5103.48	6506.87	4657.30	3042939
96	5March	6875.00	5795.31	6810.33	5449.39	3451220
108	5 March	6715.81	6246.50	6795.41	6020.90	3683571
120	6March	6307.89	6437.00	6511.85	6341.75	3734602
132	6 March	5681.08	6366.81	5994.48	6401.91	3612374
144	7 March	4745.84	6045.97	5213.46	6206.39	3314495
156	7 March	3880.25	5474.46	4313.04	5760.21	2880344
168	8 March	3273.34	4802.68	3576.79	5138.57	2411810
180	8 March	2457.49	4140.94	2865.41	4471.81	1929890
192	9 March	1830.68	3419.03	2144.08	3779.98	1439121
204	9 March	1333.21	2747.26	1581.95	3083.14	988762
216	10 March	1074.53	2155.69	1203.87	2451.47	614481
228	10 March	895.44	1704.50	984.99	1930.10	330948

To calculate K and X factors by two points method [35], a plot of the storage S, against the weighted flow XI+ (I-X) Q should be prepared and a smooth curve should be drawn through the mean position of plotted data, then parameters X and K can be determined by selecting the loop closest to a straight line as shown in the Table 4.2 and Figure 4.4. The parameters then are used as input for the hydrological model HEC-HMS, in addition to the observed hydrograph as shown in Figure 4.3. As the mentioned software depends on solving Muskingum method, after inserting the requested data and running the software, HEC-HMS gives a computed hydrograph.

Six values for X were assumed (0.15, 0.2, 0.25, 0.3, 0.35, and 0.4) then compensate at XI+ (I-X) Q to draw x-axis for Figure 4.4, while the storage shown in the Table 4.1 forms the y-axis, connecting between the points to get different loops. The loop that is closest to straight line is given by X=0.2, while the slope of this line which represent value of K parameter is K=24 hr.

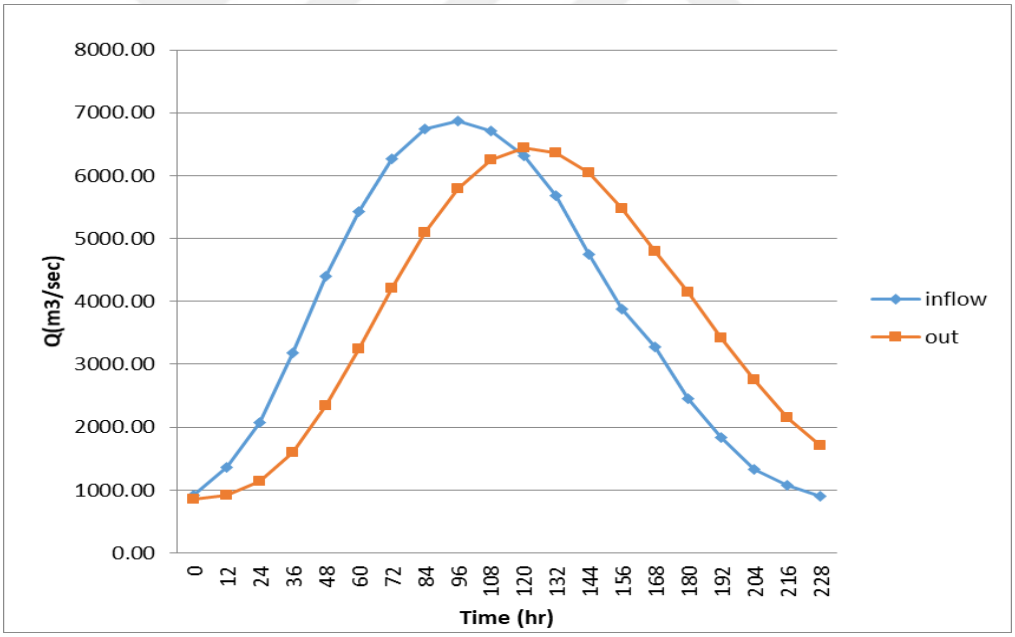

Figure 4.3 Observed inflow and outflow hydrographs

Table 4.2 Calculated value of [X*I+ (1-X)*O] according assumed value of X

[X*I+(1-X)*O]					
X=0.25	**X=0.35**	**X=0.2**	**X=0.15**	**X=0.3**	**X=0.4**
870.51	877.81	866.86	863.21	874.16	881.47
1025.07	1070.14	1002.54	980.01	1047.6	1092.67
1374.63	1467.27	1328.31	1281.99	1420.95	1513.6
1991.61	2150.56	1912.13	1832.65	2071.08	2230.04
2851.53	3057.67	2748.46	2645.39	2954.6	3160.75
3794.52	4012.9	3685.33	3576.14	3903.71	4122.09
4725.36	4931.06	4622.52	4519.67	4828.21	5033.91
5514.02	5678.24	5431.91	5349.81	5596.13	5760.35
6065.23	6173.2	6011.24	5957.26	6119.21	6227.18
6363.83	6410.76	6340.36	6316.89	6387.29	6434.22
6404.72	6391.81	6411.18	6417.63	6398.27	6385.35
6195.38	6126.81	6229.67	6263.95	6161.09	6092.52
5720.94	5590.92	5785.94	5850.95	5655.93	5525.92
5075.9	4916.48	5155.62	5235.33	4996.19	4836.77
4420.35	4267.41	4496.81	4573.28	4343.88	4190.94
3720.07	3551.73	3804.25	3888.42	3635.9	3467.56
3021.94	2863.11	3101.36	3180.78	2942.52	2783.69
2393.74	2252.34	2464.45	2535.15	2323.04	2181.64
1885.4	1777.29	1939.46	1993.52	1831.34	1723.23
1502.24	1421.33	1542.69	1583.14	1461.78	1380.88

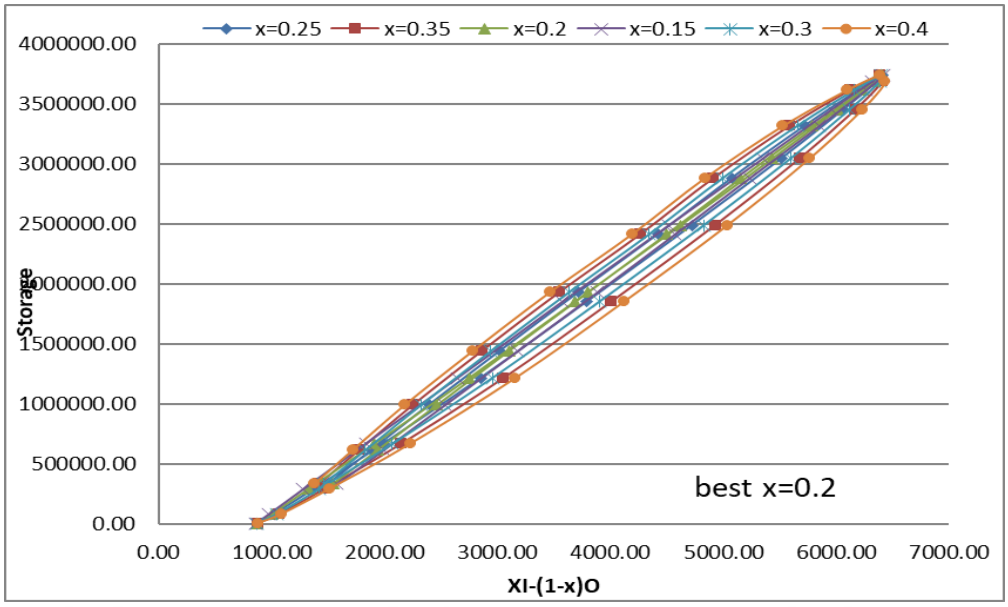

Figure 4.4 Estimation of Muskingum parameters K and X

4.2.1. HEC-HMS Application Input

The parameters K= 24 hr and X=0.2 in addition to data of flood March, 2019 in Table 4.1 has been entered to the software of HEC-HMS.

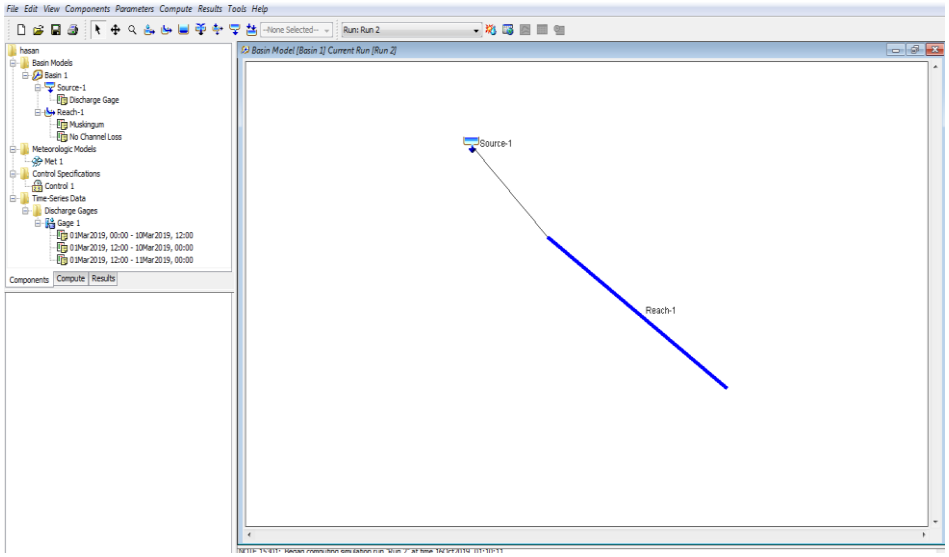

Figure 4.5 HEC-HMS interface

4.2.2. HEC-HMS Application Output

The resultant outflow hydrograph obtained by HEC-HMS flood routing is presented in Table 4.3 and Figure 4.6.

Table 4.3 Outflow hydrograph computed by HEC-HMS

Time	**HEC-HMS Outflow**
hr	**(m^3/s)**
0	-
12	1363.1
24	1396.7
36	1770.1
48	2501.1
60	3453.5
72	4435.6
84	5330.9
96	6010.8
108	6414.7
120	6538.7
132	6398.9
144	6012.6
156	5368.1
168	4630.7
180	3945.5
192	3207.1
204	2528.0
216	1946.7

For the performance check of HEC-HMS, R^2, the coefficient of determination is calculated. There are differences between the observed hydrograph and computed one, but calculating R^2 coefficient showed that the computed values are in good linear relation or in other words highly correlated with the observed one as shown in Figure 4.7 as $R^2 = 0.9883$ is very close to 1.

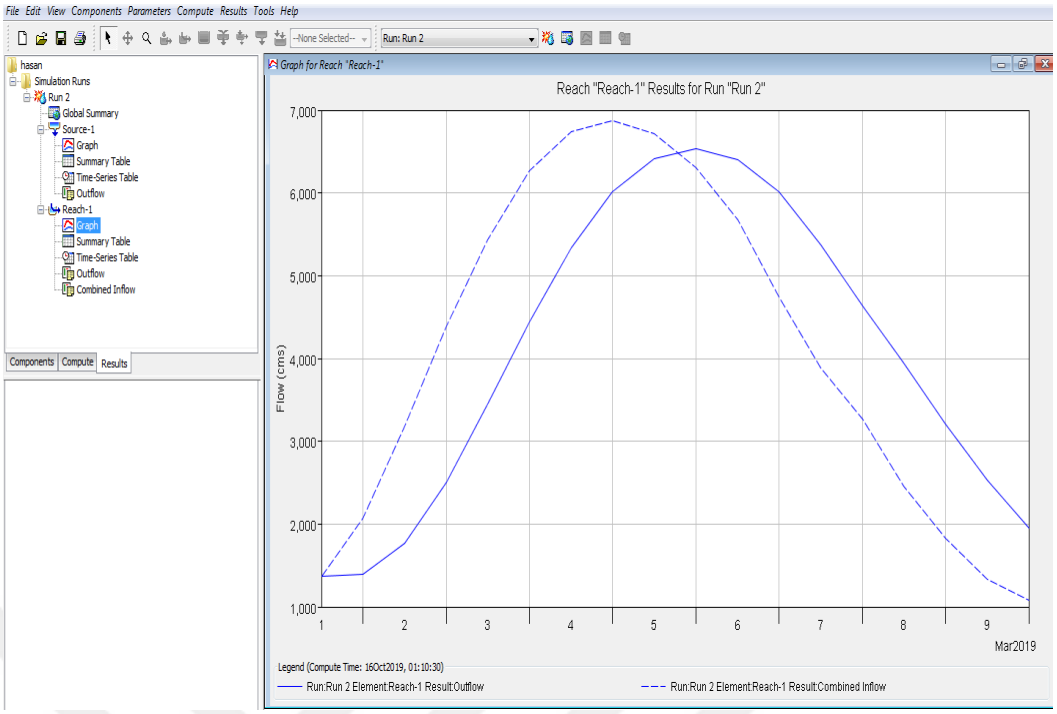

Figure 4.6 Computed hydrograph obtained from HEC-HMS

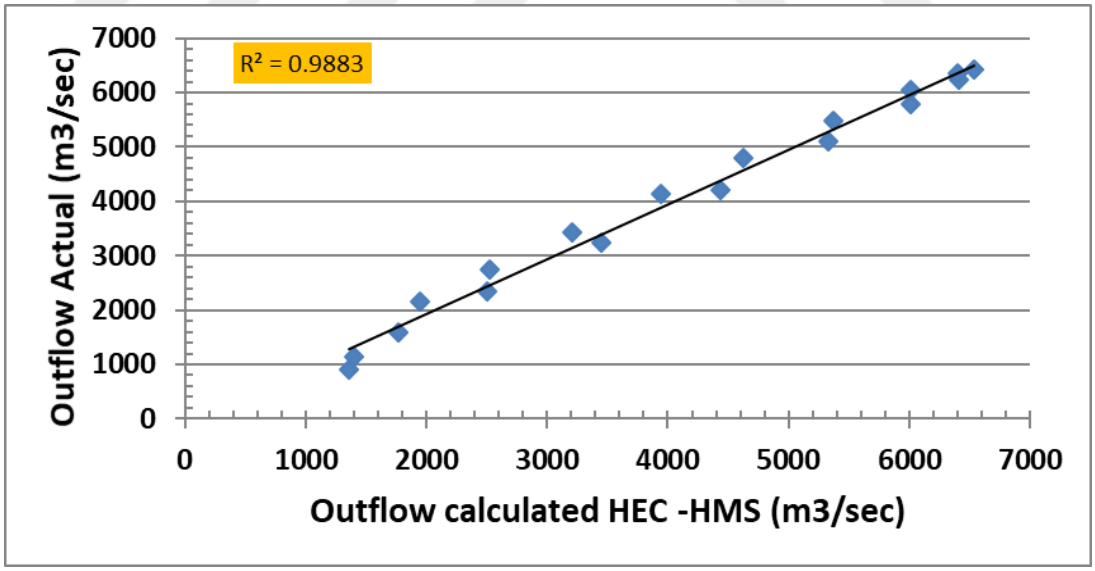

Figure 4.7 Observed outflow versus calculated HEC-HMS outflow

4.3. Part 2: Hydraulic Routing Studies

In the hydraulic routing studies with HEC-RAS necessary input data are discussed in Section 4.3.1. In this study, one-dimensional flow analysis is carried out with the software. One-dimensional flow in HEC-RAS can be successfully simulated within the channel boundaries. Whenever there is an insufficiency of the cross-sections to convey the flow, the cross-sections will be overflowed and it would be unrealistic to continue one-dimensional flow simulations. Then the problem becomes two-dimensional. However, it would also be unrealistic and impossible to simulate two-dimensional flow if the DEM of the study area cannot be implemented into the software, which is the case in this study. Considering this problem, when the one-dimensional flow simulations are carried out with HEC-RAS, it is intended to maintain the one-dimensional flow inside the channel boundaries. During the analyses, the cross-sections that are insufficient to convey the flood water are identified. In most of the cross-sections the flow capacities are sufficient for the conveyance of the given inflow hydrograph. To prevent overflow to floodplain in the identified insufficient cross-sections, levees are introduced to the cross-sections in the HEC-RAS software. This also helped to understand the parts of the Tigris River to face overflow danger to the floodplain. The necessary levee heights will be presented later in this chapter.

4.3.1. HEC-RAS Application Input

A satellite image for the study area is prepared, then the river stream is drawn on the image, as shown in Figure 4.8. The available river cross-sections obtained from Iraqi Ministry of Water Resources, Survey Authority are entered, the distance between each section, Manning roughness coefficient are entered, then the software is run to route the unsteady flow, estimate the operating time period (see Figure 4.9) for the model, then the results previewed, as shown in the Figure 4.10.

Regarding to the roughness coefficient, according to Iraqi directorates for irrigation, a range of Manning values estimated for each area depending on the nature of river bed in the selected area, so Manning coefficient value between 0.025-0.03 is adapted.

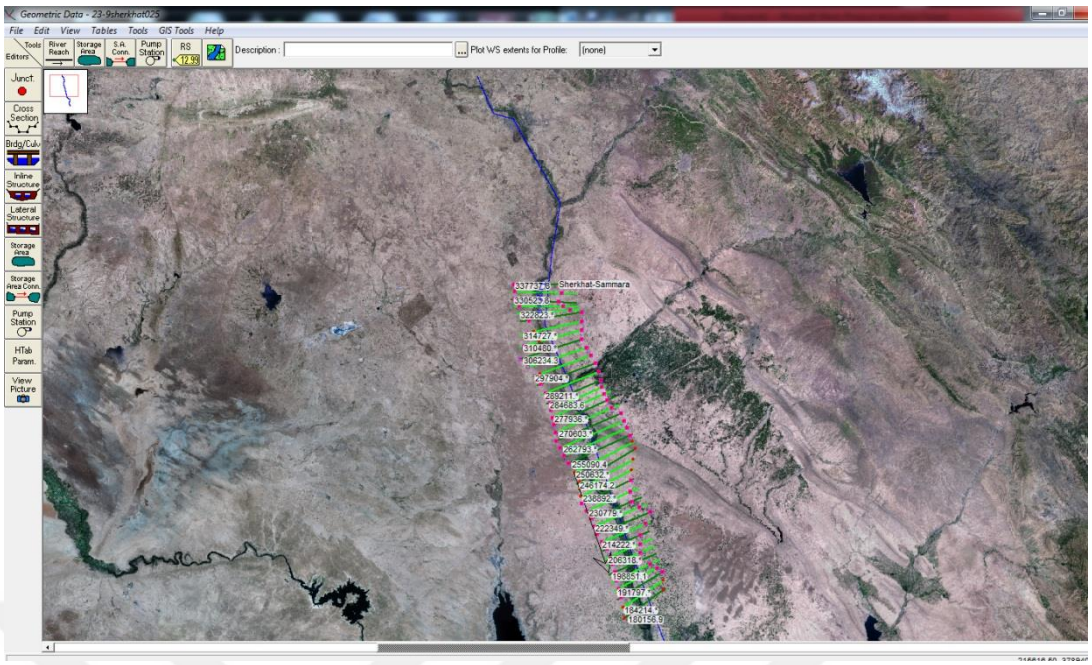

Figure 4.8 The image of the reach cross-sections

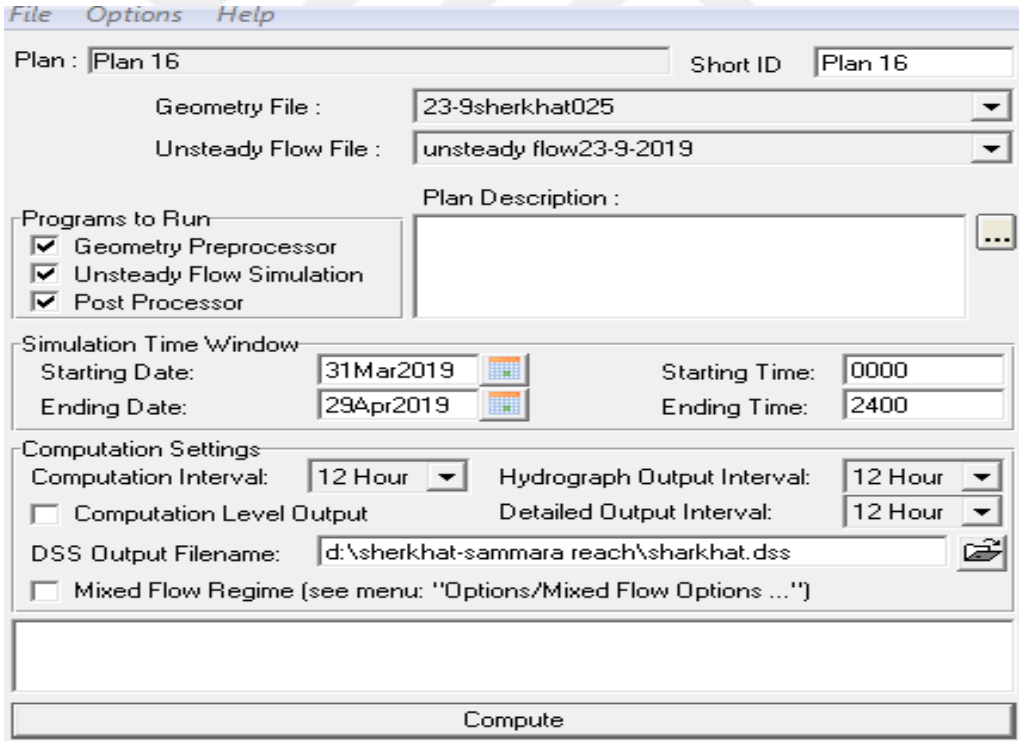

Figure 4.9 HEC-RAS operating time

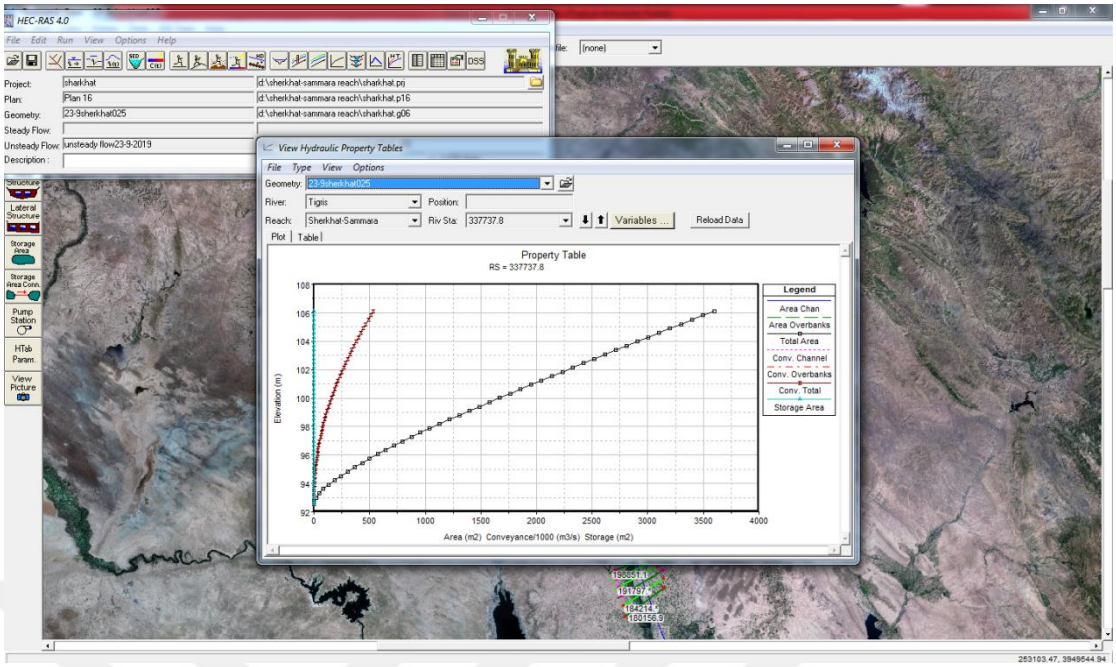

Figure 4.10 HEC-RAS interface

4.3.2. HEC-RAS Application Output

HEC-RAS depends on dividing the reach to many sections. Example cross-sections are presented in Figure 4.11 and 4.12. The other cross-sections can be found in Appendix A. The hydraulic parameters calculated by HEC-RAS are presented in Table 4.4. The resultant outflow hydrograph obtained by HEC-RAS flood routing is presented in Table 4.5.

For the performance check of HEC-RAS, R^2, the coefficient of determination is calculated. There are differences between the observed hydrograph and computed one, but calculating R^2 showed that the computed values are in good linear relation with the observed one as shown in Figure 4.13 as $R^2 = 0.9717$ is very close to 1.

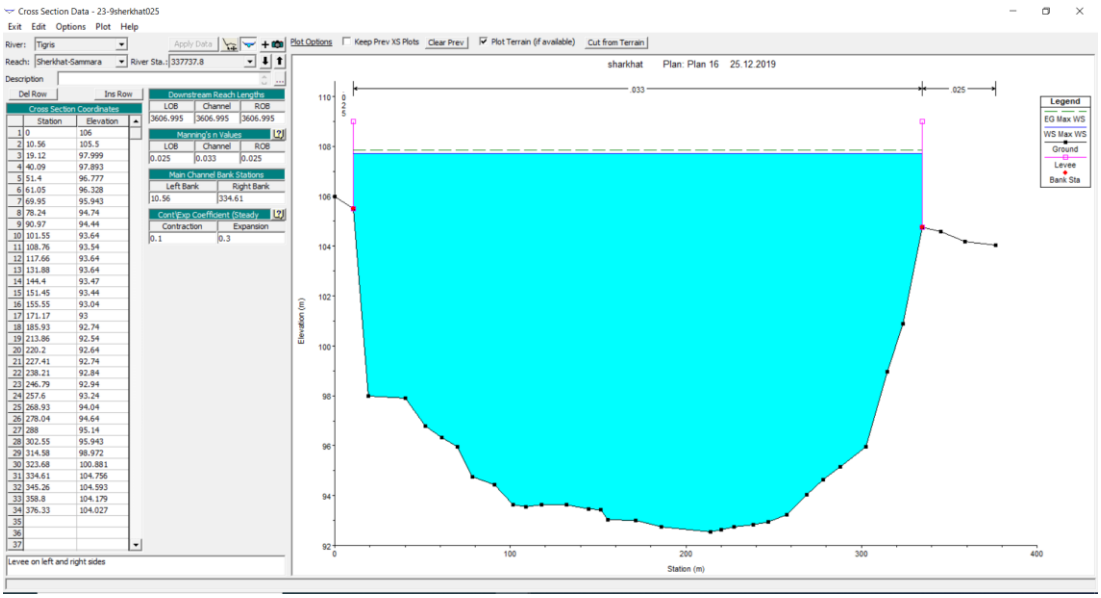

Figure 4.11 River cross-section at the upstream (Shargat station)

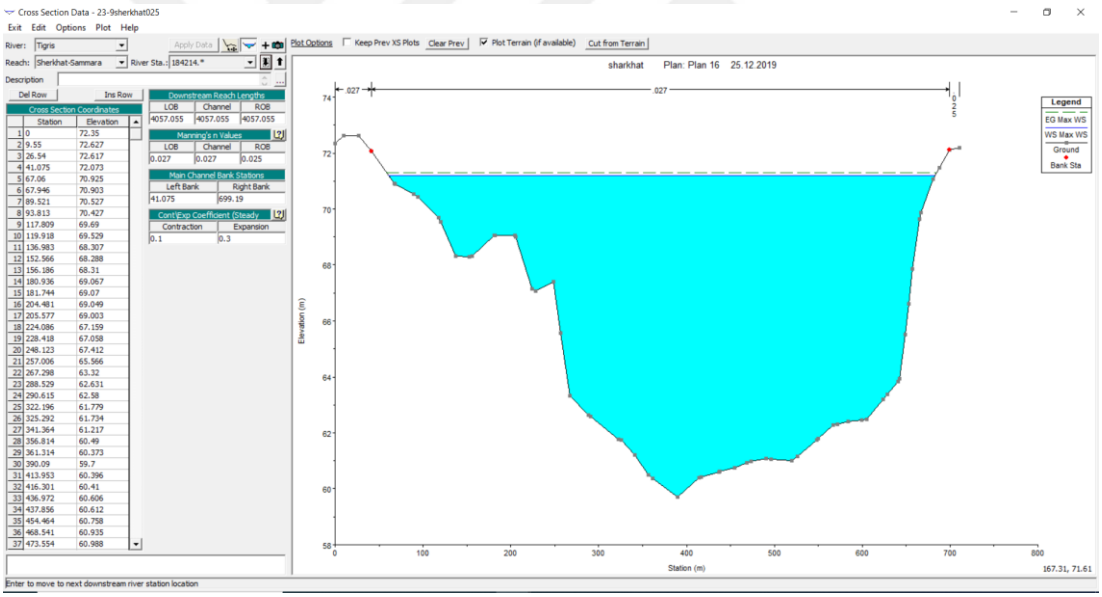

Figure 4.12 River cross-section at 153.5 km distance from the upstream

Table 4.4 Hydraulic parameters calculated by HEC-RAS

Reach	River Sta	Profile	Q Total	Min Ch El	W.S. Elev	Crit W.S.	E.G. Elev	E.G. Slope	Vel Chnl	Flow Area	Top Width	Froude # Ch
			(m3/s)	(m)	(m)	(m)	(m)	(m/m)	(m/s)	(m2)	(m)	
Sherkhat-Sammara	337737.8	Max WS	6875.00	92.54	107.72		107.86	0.000106	1.67	4118.68	324.05	0.15
Sherkhat-Sammara	334130.*	Max WS	6861.63	92.27	107.49		107.55	0.000046	1.11	6207.68	479.97	0.10
Sherkhat-Sammara	330523.8	Max WS	6843.04	92.00	107.24		107.27	0.000026	0.83	8230.58	635.88	0.07
Sherkhat-Sammara	326673.*	Max WS	6822.13	91.03	106.89		106.94	0.000030	0.95	7176.26	527.55	0.08
Sherkhat-Sammara	322823.*	Max WS	6804.67	90.05	106.54		106.61	0.000044	1.14	5946.62	419.21	0.10
Sherkhat-Sammara	318973.9	Max WS	6791.13	89.08	106.06		106.18	0.000077	1.51	4504.73	310.88	0.13
Sherkhat-Sammara	314727.*	Max WS	6779.25	88.64	105.25		105.39	0.000092	1.64	4163.76	311.21	0.14
Sherkhat-Sammara	310480.*	Max WS	6767.66	88.19	104.07		104.23	0.000120	1.81	3765.12	311.55	0.16
Sherkhat-Sammara	306234.3	Max WS	6727.70	87.75	102.09		102.32	0.000196	2.12	3164.31	311.88	0.20
Sherkhat-Sammara	302069.*	Max WS	6727.08	86.43	100.10		100.27	0.000163	1.84	3680.97	375.75	0.18
Sherkhat-Sammara	297904.*	Max WS	6725.64	85.11	98.70		98.83	0.000126	1.57	4302.04	439.61	0.16
Sherkhat-Sammara	293740.0	Max WS	6723.39	83.79	97.78		97.87	0.000090	1.32	5095.43	503.48	0.13
Sherkhat-Sammara	289211.*	Max WS	6720.66	82.41	96.97		97.10	0.000110	1.58	4260.41	417.48	0.16
Sherkhat-Sammara	284683.6	Max WS	6718.25	81.03	96.22		96.41	0.000131	1.94	3479.59	331.49	0.19
Sherkhat-Sammara	281310.*	Max WS	6716.32	80.02	95.59		95.80	0.000204	2.07	3247.40	416.89	0.24
Sherkhat-Sammara	277936.*	Max WS	6713.73	79.01	94.61		94.90	0.000330	2.38	2816.86	444.62	0.30
Sherkhat-Sammara	274563.1	Max WS	6711.18	78.00	93.79		94.04	0.000179	2.22	3019.30	296.83	0.22
Sherkhat-Sammara	270603.*	Max WS	6708.19	77.50	93.00		93.27	0.000212	2.30	2914.10	368.30	0.26
Sherkhat-Sammara	266644.4	Max WS	6705.31	77.00	91.94		92.33	0.000264	2.74	2443.55	229.43	0.27
Sherkhat-Sammara	262793.*	Max WS	6703.10	76.33	90.97		91.39	0.000223	2.86	2341.59	215.81	0.26
Sherkhat-Sammara	258941.*	Max WS	6700.95	75.67	90.05		90.51	0.000236	2.99	2244.75	201.30	0.29
Sherkhat-Sammara	255090.4	Max WS	6698.94	75.00	88.86		89.39	0.000345	3.21	2088.27	186.07	0.31
Sherkhat-Sammara	250632.*	Max WS	6696.65	73.56	87.11		87.71	0.000408	3.44	1946.77	192.24	0.35
Sherkhat-Sammara	246174.2	Max WS	6694.13	72.12	85.02		85.66	0.000512	3.54	1890.60	200.72	0.37
Sherkhat-Sammara	242533.*	Max WS	6691.48	71.41	83.46		83.96	0.000420	3.13	2140.95	238.67	0.33
Sherkhat-Sammara	238892.*	Max WS	6687.73	70.71	82.17		82.56	0.000348	2.78	2403.95	279.02	0.30
Sherkhat-Sammara	235251.7	Max WS	6682.30	70.00	81.10		81.41	0.000285	2.47	2706.84	324.53	0.27
Sherkhat-Sammara	230779.*	Max WS	6671.87	68.67	80.29		80.45	0.000142	1.78	3756.00	439.97	0.19
Sherkhat-Sammara	226306.7	Max WS	6655.78	67.33	79.95		80.02	0.000049	1.13	5866.35	602.07	0.12
Sherkhat-Sammara	222349.*	Max WS	6639.76	66.33	79.76		79.83	0.000046	1.17	5659.49	519.48	0.11
Sherkhat-Sammara	218392.3	Max WS	6625.85	65.33	79.56		79.64	0.000048	1.27	5204.62	436.90	0.12
Sherkhat-Sammara	214222.*	Max WS	6613.75	64.29	79.24		79.37	0.000069	1.55	4272.10	347.36	0.14
Sherkhat-Sammara	210051.7	Max WS	6604.51	63.25	78.54		78.76	0.000132	2.09	3160.16	257.82	0.19
Sherkhat-Sammara	206318.*	Max WS	6597.62	63.00	77.55		77.79	0.000146	2.14	3077.46	269.27	0.20
Sherkhat-Sammara	202584.*	Max WS	6590.91	62.75	76.21		76.48	0.000196	2.29	2883.21	280.73	0.23
Sherkhat-Sammara	198851.1	Max WS	6584.68	62.50	74.11		74.48	0.000353	2.69	2445.26	292.18	0.30
Sherkhat-Sammara	195324.*	Max WS	6577.44	61.67	72.62		72.81	0.000233	1.95	3368.95	494.07	0.24
Sherkhat-Sammara	191797.*	Max WS	6548.33	60.83	71.99		72.10	0.000149	1.52	4300.97	656.50	0.19
Sherkhat-Sammara	188271.0	Max WS	6547.97	60.00	71.64		71.72	0.000070	1.19	5500.79	692.42	0.13
Sherkhat-Sammara	184214.*	Max WS	6547.42	59.70	71.19		71.31	0.000132	1.53	4266.56	621.70	0.19
Sherkhat-Sammara	180156.9	Max WS	6546.94	59.40	69.69	65.73	70.04	0.000490	2.60	2523.31	442.09	0.34

Table 4.5 Outflow hydrograph computed by HEC-RAS

Time (hr)	HEC-RAS Outflow (m^3/s)
0	-
12	1437.12
24	1530.48
36	1825.45
48	2541.42
60	3620.39
72	4482.05
84	5774.08
96	6226.82
108	6541.62
120	6600.29
132	6468.57
144	5904.75
156	5287.65
168	4487.52
180	3712.99
192	3144.82
204	2662.77
216	1985.10

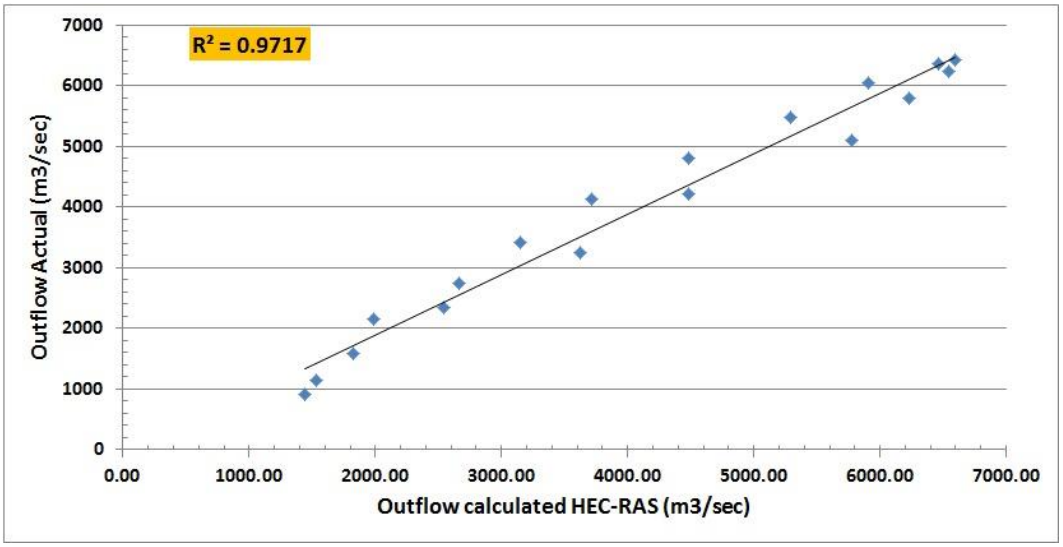

Figure 4.13 Observed outflow versus calculated HEC-RAS outflow

4.4. Discussion and Comparison of the Hydrologic and Hydraulic Routing Results

Together with the inflow and observed outflow hydrographs, the results obtained from HEC-HMS and HEC-RAS software are presented in Figure 4.14 and Table 4.6. As shown in the table the discharges of the observed hydrograph are lower than the calculated hydrographs up to 144 hr, then they become higher. The percent differences of HEC-HMS and HEC-RAS outflow values from observed outflow values are also presented. As seen in the table, the highest differences are observed at the beginning of the outflow hydrograph. For a flood event, the peak discharge of the hydrograph is of great importance. When the peak discharges are compared, it is seen that HEC-HMS outflow peak is 6538.7 m^3/s, HEC-RAS outflow peak is 6600.29 m^3/s where the observed outflow peak is 6437 m^3/s. The percent differences of the peak discharges from observed value are found to be 1.58% and 2.54% for HEC-HMS and HEC-RAS, respectively. Compared to the average differences, the peak discharges are found to be relatively closer to the observed values.

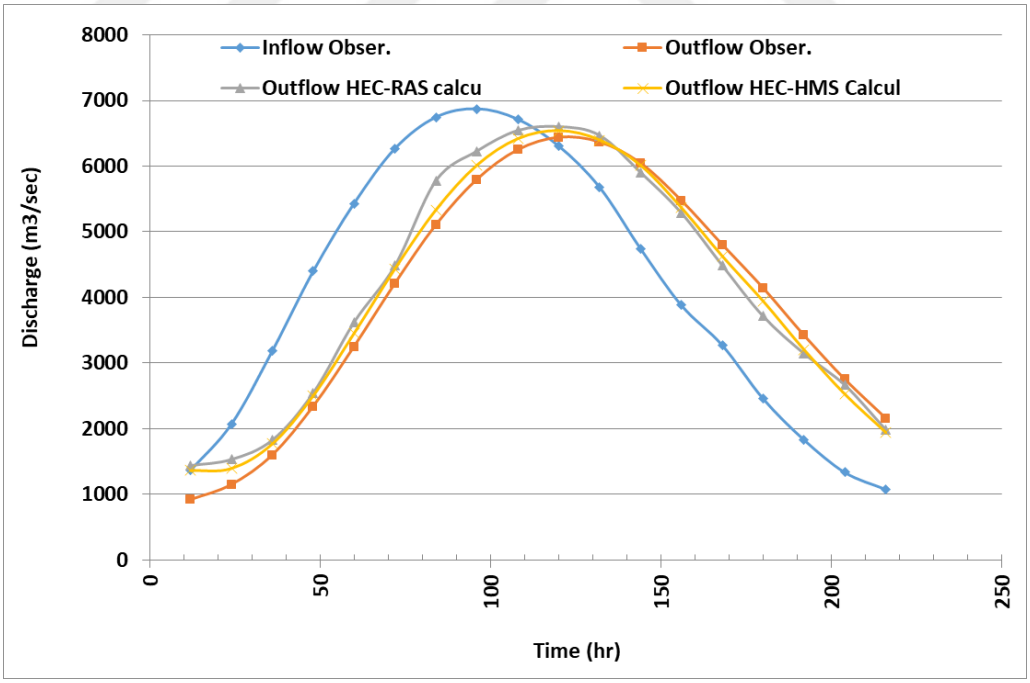

Figure 4.14 Inflow versus observed, HEC-HMS, and HEC-RAS outflow hydrographs

Table 4.6 Comparison of observed and calculated outflow hydrographs and percent differences from observed outflow

Time (hr)	**I (m^3/s)**	**Q (m^3/s) (obs.)**	**Q (m^3/s) (HEC -HMS)**	**Q (m^3/s) (HEC -RAS)**	**% diff. (HEC -HMS)**	**% diff. (HEC -RAS)**
0	925.29	852.25				
12	1363.06	912.41	1363.10	1437.12	49.40	57.51
24	2069.46	1143.02	1396.70	1530.48	22.19	33.90
36	3183.79	1594.21	1770.10	1825.45	11.03	14.50
48	4397.61	2336.17	2501.10	2541.42	7.06	8.79
60	5432.34	3248.58	3453.50	3620.39	6.31	11.45
72	6268.09	4211.12	4435.60	4482.05	5.33	6.43
84	6745.66	5103.48	5330.90	5774.08	4.46	13.14
96	6875.00	5795.31	6010.80	6226.82	3.72	7.45
108	6715.81	6246.50	6414.70	6541.62	2.69	4.72
120	6307.89	6437.00	6538.70	6600.29	1.58	2.54
132	5681.08	6366.81	6398.90	6468.57	0.50	1.60
144	4745.84	6045.97	6012.60	5904.75	-0.55	-2.34
156	3880.25	5474.46	5368.10	5287.65	-1.94	-3.41
168	3273.34	4802.68	4630.70	4487.52	-3.58	-6.56
180	2457.49	4140.94	3945.50	3712.99	-4.72	-10.33
192	1830.68	3419.03	3207.10	3144.82	-6.20	-8.02
204	1333.21	2747.26	2528.00	2662.77	-7.98	-3.08
216	1074.53	2155.69	1946.70	1985.10	-9.69	-7.91

A summary table (see Table 4.7) is prepared for the comparison of peak discharge values and time to peak values of all hydrographs, i.e. inflow, observed outflow, HEC-HMS outflow, and HEC-RAS outflow. In addition, the attenuation and translation of the outflow hydrographs are also presented in the table. As can be seen from Table 4.7 and Figure 4.14, time to peak values of all outflow hydrographs are the same, i.e. 120 hr. This has resulted in 24 hr translation in all outflow hydrographs. It is obvious that both hydrologic and hydraulic routing are very successful in predicting the temporal variation of discharges at a downstream location, with a given inflow hydrograph.

Table 4.7 Comparison of observed and calculated attenuation and translation

Hydrograph	Peak Discharge (m^3/s)	Time to Peak (hr)	Attenuation (m^3/s)	Translation (hr)
Inflow	6875.00	96		
Outflow - Observed	6437.00	120	438.00	24
Outflow - HEC-HMS	6538.70	120	336.30	24
Outflow - HEC-RAS	6600.29	120	274.71	24

The attenuation of outflow hydrographs is differing to some extent due to differences in the peak discharges as already mentioned above. Both hydrologic and hydraulic routing methods are predicting the peak discharges higher than the observed outflow peak. First of all, overestimation of peak discharges in a severe flood event is somehow favorable rather than underestimation, since underestimation may result in further adverse effects on the flood inundation areas. At this point, HEC-HMS and HEC-RAS results must be discussed separately. With the available data, a lumped hydrologic routing simulation could be carried out using HEC-HMS software. The study reach is considered as a homogeneous reach without any change in the K and X parameters. However, a 158 km distance is very long to treat as a homogeneous reach. That is why HEC-RAS results at the beginning were thought to be more accurate than HEC-HMS results with the available data. When it comes to HEC-RAS results, it is observed that the discharges are further higher than the HEC-HMS results. At first glance, it seems HEC-HMS predictions are relatively closer to the observed discharges compared to that of HEC-RAS. However, it is very important to remember that the insufficient cross-sections to convey the flood water were altered by the addition of levees. It means, in the natural course of the Tigris River, some of the flood water is overflowing to the floodplain where the cross-sections are insufficient to convey a flood hydrograph with a peak discharge of 6875 m^3/s as simulated in this study. On the other hand, the levees implemented in this study prevented the overflowing, so all flood water is routed towards downstream without any loss to floodplain. That is why, obtaining higher discharge values in HEC-RAS simulation compared to observed outflow is an expected result. Furthermore, the recommended Manning roughness values are adapted to cross-sections in a given

range. A detailed survey for the roughness characteristics of the channel and bed slopes may also increase the simulation success of HEC-RAS software.

Although the discharge values of observed, HEC-HMS, and HEC-RAS outflows do not 100% match as mentioned above, it is obvious that all three hydrographs are following the same trend as can be seen in Figure 4.14. Another correlation check is carried out to determine the R^2 of HEC-HMS / HEC-RAS outflows, which have been previously done for HEC-HMS / observed and HEC-RAS / observed outflow values. As presented in Figure 4.15, HEC-HMS and HEC-RAS outflows are also in good linear relation with $R^2 = 0.9772$ which is very close to 1.

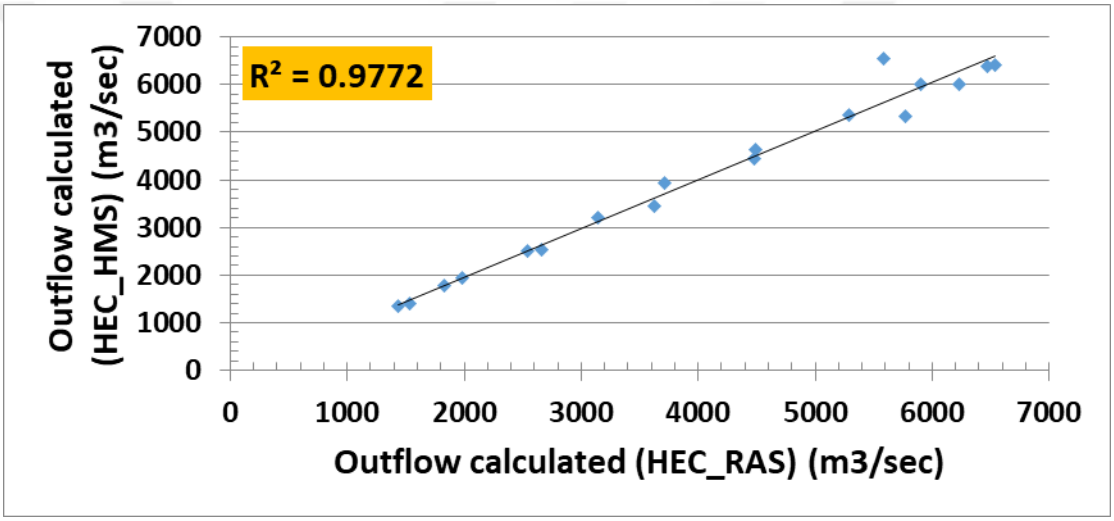

Figure 4.15 HEC-HMS outflow versus HEC-RAS outflow

As mentioned earlier, in the HEC-RAS simulations levees are introduced to maintain one-dimensional flow within the channel boundaries. Table 4.8 presents the cross-section distances from the most upstream station Shargat and minimum necessary levee heights at the left and right bank in the flow direction. As can be seen from the table, the first 56 km part at the upstream of the reach has a need of levee at the left bank with a height of 0.70 – 9.53 m and at the right bank with a height of 2.80 – 10.17 m. At the downstream part of the reach, the need of levee height at the left bank is 0.86 – 7.24 m and at the right bank is 1.95 – 7.64 m. This implies the importance of levee construction to prevent severe flood inundation in the study area.

Table 4.8 Minimum necessary levee heights at the left and right bank of the reach

Distance from upstream (km)	Left bank levee height (m)	Right bank levee height (m)	Distance from upstream (km)	Left bank levee height (m)	Right bank levee height (m)
0.0	2.22	2.96	82.6	-	-
3.6	5.88	6.56	87.1	-	-
7.2	9.53	10.13	91.6	-	-
11.1	9.47	10.15	95.2	-	-
14.9	9.41	10.17	98.8	-	-
18.8	9.23	10.06	102.5	-	-
23.0	9.41	9.75	107.0	-	-
27.3	9.50	9.07	111.4	-	2.56
31.5	8.24	7.59	115.4	0.86	3.37
35.7	7.46	6.68	119.3	1.68	4.17
39.8	7.03	6.35	123.5	4.65	6.10
44.0	6.28	6.51	127.7	7.24	7.64
48.5	4.86	6.33	131.4	7.24	7.47
53.1	3.38	6.22	135.2	6.89	6.96
56.4	0.70	2.80	138.9	5.78	5.67
59.8	-	-	142.4	2.02	1.95
63.2	-	-	145.9	-	-
67.1	-	-	149.5	-	-
71.1	-	-	153.5	-	-
74.9	-	-	157.6	-	-
78.8	-	-	-	-	-

CHAPTER 5

CONCLUSIONS AND RECOMMENDATIONS

5.1. Conclusions

In this study hydrologic and hydraulic flood routing is performed on a 150 km reach on the Tigris River from Al Shargat to the Samarra Dam by using HEC-HMS and HEC-RAS software, respectively. The inflow hydrograph at Shargat station is the common input to both software. As a result of the flood routing simulations with both software, the outflow hydrograph at Samarra station is calculated. The conclusions are as follows:

- The distributed hydraulic routing method is mathematically more complicated than the lumped hydrologic routing method. It obtains the results by solving simultaneously the complete unsteady Saint-Venant equations throughout the reach. Before performing any flood routing simulation, it is expected to obtain better estimation of outflow hydrograph with HEC-RAS software.
- The peak discharge of the inflow hydrograph and time to peak are 6875.00 m^3/s and 96 hr, respectively. Same values are 6437.00 m^3/s - 120 hr for the observed outflow hydrograph, 6538.70 m^3/s - 120 hr for the HEC-HMS outflow hydrograph, and 6600.29 m^3/s - 120 hr for the HEC-RAS outflow hydrograph.
- Time to peak values of outflow hydrograph is estimated with HEC-HMS and HEC-RAS exactly the same as the observed outflow hydrograph, i.e. the translation is calculated with both software similar to that of observed hydrograph. This proves the success of both methods in predicting the temporal variation of discharges of a routed hydrograph.
- The peak discharges are 1.58% and 2.54% higher in HEC-HMS and HEC-RAS outflow, respectively compared the observed outflow. The lack of detailed data to perform semi-distributed hydrologic modeling is thought to be the reason of this difference in HEC-HMS simulations. As mentioned earlier, HEC-RAS

simulations were expected to result in a better estimation of routed outflow hydrograph compared to HEC-HMS. Obtaining rather relatively worse estimation are linked to the cross-section alteration in HEC-RAS by adding levees to maintain one-dimensional flow within the channel boundaries. With the added levees to the cross-sections where the flow capacity is insufficient to convey flood hydrograph, the overflowing of flood water to the floodplain is prevented. This is expected to be the major reason of obtaining higher discharge values with HEC-RAS compared to the observed outflow.

- The correlation between the outflow hydrographs are tested by calculating the R^2 values. The R^2 values of observed outflow – HEC-HMS outflow, observed outflow – HEC-RAS outflow, and HEC-HMS outflow – HEC-RAS outflow are 0.9883, 0.9717, and 0.9772, respectively. Since all R^2 values are very close to 1, it is concluded that observed and estimated outflow hydrographs are in good linear relation.
- The cross-sections up to 56 km distance and the cross-sections at 115 – 142 km distance from the Shargat station at the upstream of the study reach are found to be insufficient by their flow capacity. The necessary height of levees to those cross-sections are determined during HEC-RAS simulations in the range of approximately 1 – 10 m. This information will be beneficial for the implementation of necessary precautions against floodplain inundation.
- The results of the presented research indicate that if the river reach has modest values of geometric data like bed slope and roughness coefficient, HEC-RAS model result is more accurate in order to be utilized in design projects of unmanaged catchments.
- Coupling of hydrological and hydraulic models can form an important tool for the management of flood control and for real-time simulation of inundation to prevent or reduce damage in terms of lives, property, and infrastructure.

5.2. Recommendations

The present study is performed to apply both hydrologic and hydraulic routing methods with the aid of suitable software programs to a reach on the Tigris River using available data. Some limitations arose in the current study due to lack of

detailed data. Recommendations for the future studies to overcome those limitations, are as follows:

- Although the geographical importance of the study area in terms of population and agriculture, within the study reach on the Tigris River which is about 158 km, there are no observation stations other than Shargat and Samarra stations to predict the discharge and elevation of water in this specific area. Detailed survey of river sections with increased number of observation stations is the foremost recommendation for further studies in this specific area. To get higher accuracy in utilization of flood routing software in the upcoming researches, increased data availability is highly recommended.
- For further research on the flood routing in the study area, reservoir routing at the Samarra Dam can be carried out.
- Hydrologic flood routing studies can be simulated in more detail with necessary detailed meteorological data, if available. Furthermore, different floods may be analyzed when sufficient data become available, to make the forecasting more robust and reliable.
- More accurate Manning roughness coefficient values may be obtained through detailed bed topography and bed material data.
- Different solution methods can be applied in HEC-HMS software when sufficient data become available.
- When data become available, two-dimensional flood modeling can be performed using HEC-RAS 2D.

REFERENCES

[1] I.R. Karim, “Hydrologic and hydraulic flood routing in the Tigris River between Mosul and Biji, A comparison study”, M.Sc. thesis, University of Technology, Iraq, 1998.

[2] D.A. Barry and K. Bajracharya, "On the Muskingum-Cunge flood routing method." *Environment International*, vol. 21(5), pp. 485-490, 1995.

[3] F.E. Hicks and T. Peacock, “Suitability of HEC-RAS for flood forecasting”, *Canadian Water Resources Journal*, vol. 30(2), pp. 159-17, 2015.

[4] P.B. Bedient and C.W. Huber, *Hydrology and Floodplain Analysis*, Rice University-University of Florida, 1988.

[5] J. Sun, “Hydrologic and hydraulic model development for flood mitigation and routing method comparison in Soap Creek Watershed, Iowa”, M.Sc. thesis, University of Iowa, 2015.

[6] K. Fung, “Assessment of Channel Routing for WRIMS CalLite Application; North of the Sacramento Delta”, University of California, Davis, 2009.

[7] D.N. Kumar, F. Baliarsingh, K.S. Raju, "Extended Muskingum method for flood routing.", *Journal of Hydro-environment Research*, vol. 5(2), pp. 127-135, 2011.

[8] R. Barat, H.A. Gholam, R. Sajjad, “Flood Routing of an Unmanaged River Basin Using Muskingum–Cunge Model; Field Application and Numerical Experiments”, *Caspian Journal of Applied Sciences Research*, vol. 2(6) , pp. 08-20, 2013.

[9] Q.H. Mohammad, “Calculating the Coefficients of Muskingum and Muskingum-Cunge Methods for a reach from Shat Al-Hilla River”, *Journal of University of* Babylon, vol. 22(4), 2014.

[10] Y.D. Twumasi, R.J. Ayer, E.M. Osei, “Computing Flood Volume of Dikpe Catchment using HEC-HMS”, *Global Journal of Human-Social Science: B Geography, Geo-Sciences, Environmental Science & Disaster Management*, vol. 15(2), 2015.

[11] S. Haque, A.K.M.S. Islam, G.M.T. Islam, M. Salehin, M.J.U. Khan, “Event based flash flood simulation at Sunamganj using HEC-HMS”, 6th International Conference on Water & Flood Management, 2017.

[12] L. Sinha, S.M. Narulkar, A.K.Chowdhary, “Analysis of Flood Routing in Channels of Ban Sagar Project: A Case Study”, International Conference on “Recent Advances in Interdisciplinary Trends in Engineering & Applications, 2019.

[13] K.A. McKay, “Hydraulic Flood Routing with Minimal Channel Data”, M.Sc. thesis, University of Alberta, 1997.

[14] A. Havel, “Hydrologic and Hydraulic Response to Wildfire in The Upper Cache la Poudre Watershed Using a SWAT and HEC-RAS Model Cascade”, M.Sc. thesis, Colorado State University, 2015.

[15] D.T. Mai and F. De Smedt, “A Combined Hydrological and Hydraulic Model for Flood Prediction in Vietnam Applied to the Huong River Basin as a Test Case Study”, *Water*, vol.9(11), 2017.

[16] A. Husain, “Flood Modelling by Using HEC-RAS”, *International Journal of Engineering Trends and Technology (IJETT)*, vol. 50(1), 2017.

[17] M.Shayannejad, K.O. Ali-Askari, S. Eslamian, V.P. Singh, N.R. Dalezios, “Analyzing of Flow in Open Channels Networks Using HEC-RAS”, *Journal of Ecology & Natural Resources*, vol. 2(4), 2018.

[18] D.R. Maidment, *Handbook of Hydrology*, New York: McGraw-Hill, 1993.

[19] “Hydrology Studio”, Internet: www.hydrologystudio.com, [November 2019].

[20] V.T. Chow, *Handbook of Applied Hydrology*, New York: McGraw-Hill Book Company, 1964.

[21] V.M. Ponce, *Engineering Hydrology Principles and Practice*, Englewood Cliffs, NJ: Prentice Hall, 1989.

[22] R.K. Linsley Jr, M.A. Kohler, J.L.H. Paulhus, *Hydrology for Engineers*, New York: McGraw-Hill Book Company, 1975.

[23] T. O'Donnell, “A direct three-parameter Muskingum procedure incorporating lateral inflow”, *Hydrological Sciences Journal,* vol. 30(4), pp. 479-496, 1985.

[24] J. Cunge, *Practical aspects of computational river hydraulics*, London: Pitman Publishing Ltd., 1980.

[25] US Army Corps of Engineers Hydrologic Engineering Center, *HEC-RAS, River Analysis System Hydraulic Reference Manual*, 2016.

[26] J. Khadka and J. Bhaukajee, “Rainfall-Runoff Simulation and Modelling Using HEC-HMS and HEC-RAS Models: Case Studies from Nepal and Sweden Hydrologic and Hydraulic Model Development for Flood Inundation Mapping of Kävlinge and Kankai River Basin”, M.Sc. thesis, Lund University, Sweden, 2018.

[27] N.P. Gautama, “Flow routing with Semi-distributed hydrological model HEC-HMS in case of Narayani River Basin”, *Journal of the Institute of Engineering,* vol. 10(1), pp. 45-58, 2014.

[28] R. Peters, G. Schmitz, J. Cullmann, “Flood routing modelling with Artificial Neural Networks”, *Advances in Geosciences,* vol. 9, pp.131-136, 2006.

[29] B.G. Tassew, M.A. Belete, K. Miegel, “Application of HEC-HMS Model for Flow Simulation in the Lake Tana Basin: The Case of Gilgel Abay Catchment, Upper Blue Nile Basin, Ethiopia”, *Hydrology*, vol. 6(1), 2019.

[30] L.I Ntoanidis and M.A. Mimikou, “Intercomparison of the lumped versus semi-distributed HEC-HMS hydrological model in the Kalamas river basin”, *Proceedings of the 13th International Conference of Environmental Science and Technology,* 2013.

[31] V. Te Chow, R. Maidment, L.W. Mays, “Applied Hydrology”, *Water Resources Handbook*, 1988.

[32] “CVE341-Water Resources Lecture Notes 4: Chapter 13: Momentum Principles in Open Channels”, Internet: slideplayer.com/slide/3268872/, [February 2020].

[33] “Samarra Barrage”, Internet: en.wikipedia.org/wiki/Samarra_Barrage, [February 2020].

[34] BBC News, Internet: www.bbc.com/news, [September 2019]

[35] M.A. Gill “Flood routing by the Muskingum method.”, *Journal of Hydrology*, vol. 36(3–4), pp. 353–363, 1978.

APPENDIX A

HEC-RAS CROSS-SECTIONS OF THE STUDY REACH

Here, the cross-sections of the study reach on the Tigris River used in HEC-RAS software are presented. These cross-sections involve the original sections obtained from Iraqi Ministry of Water Resources and the cross-sections interpolated by the software HEC-RAS.

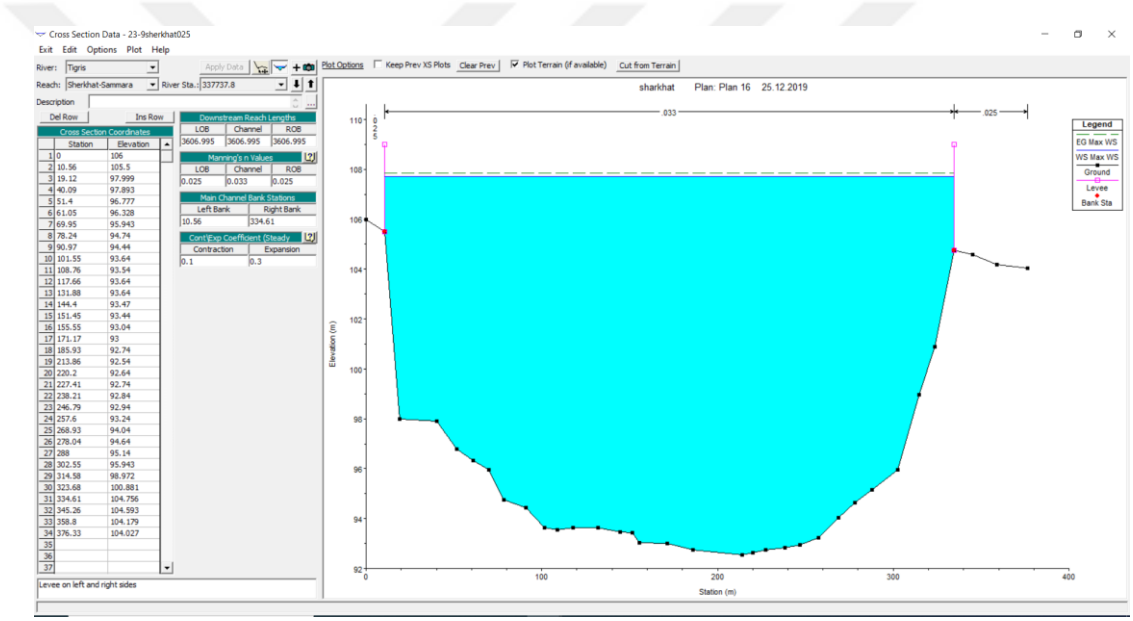

Figure A.1 River cross-section at Shargat Station

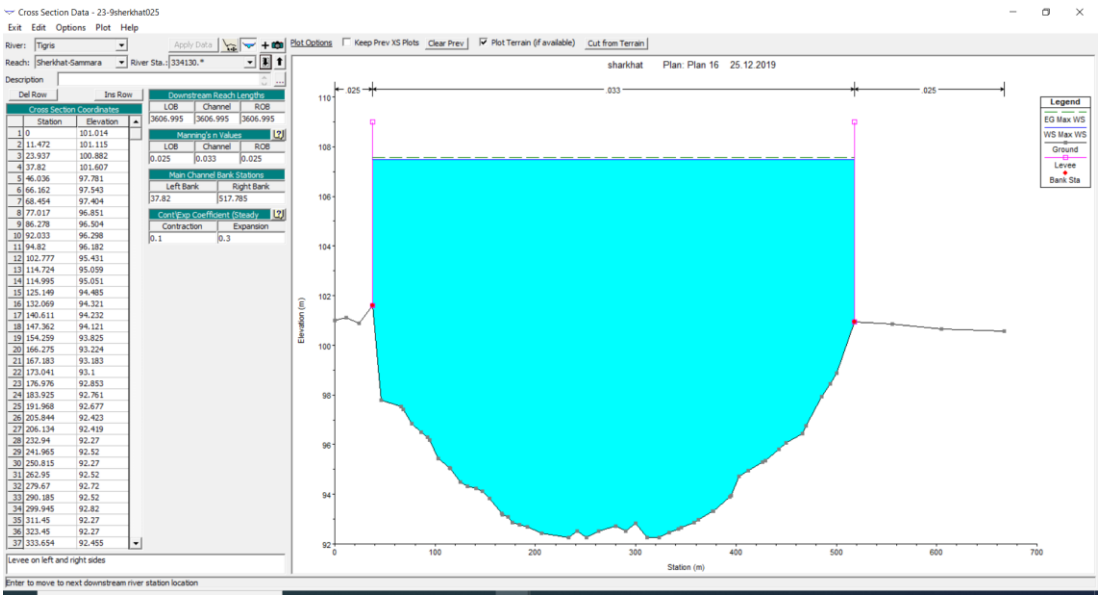

Figure A.2 River cross-section at 3.6 km distance from the upstream

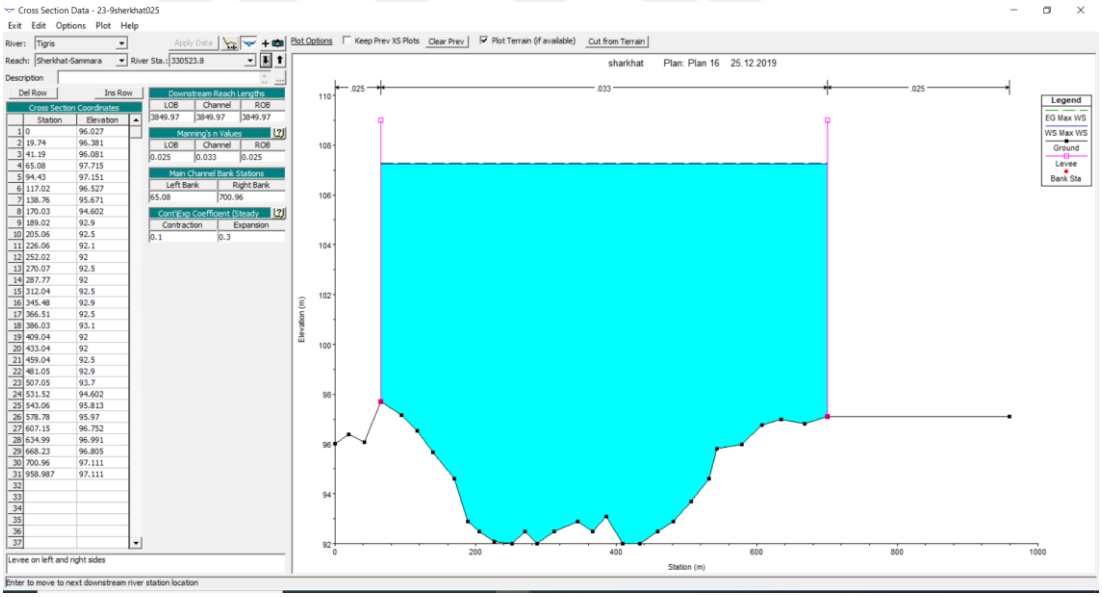

Figure A.3 River cross-section at 7.2 km distance from the upstream

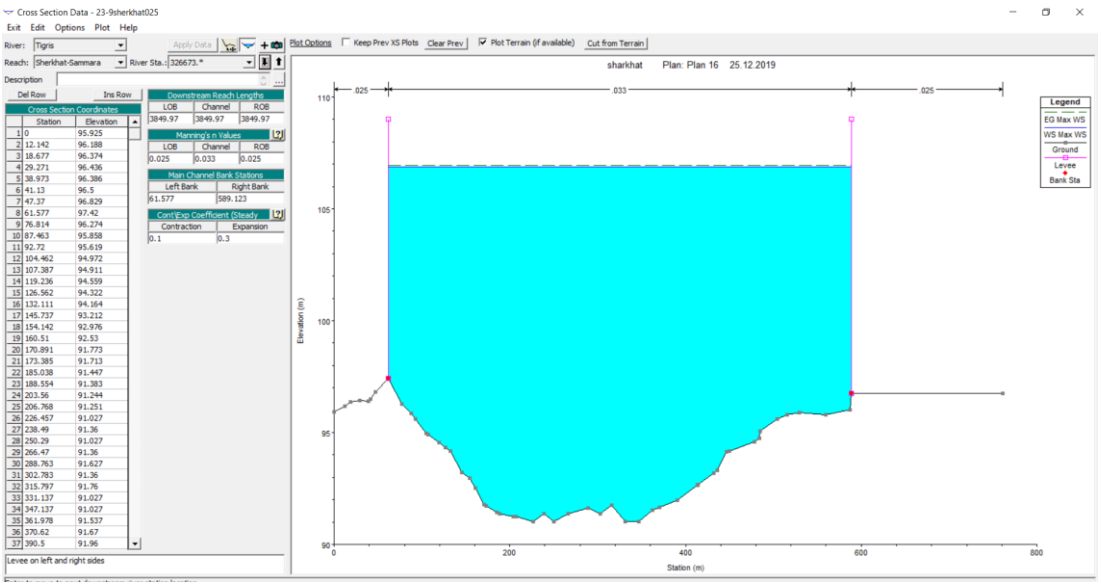

Figure A.4 River cross-section at 11.1 km distance from the upstream

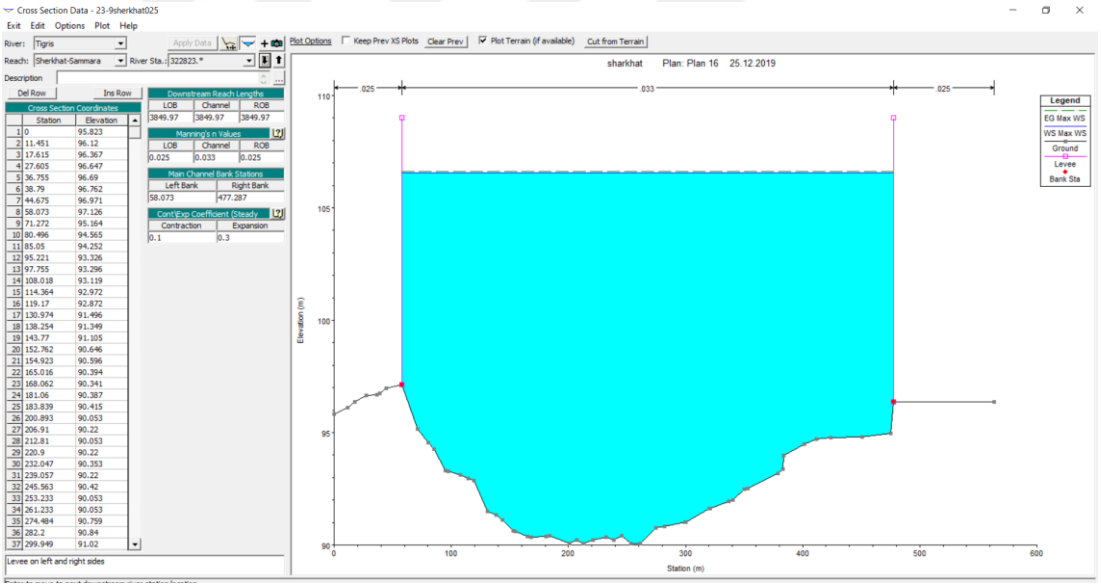

Figure A.5 River cross-section at 14.9 km distance from the upstream

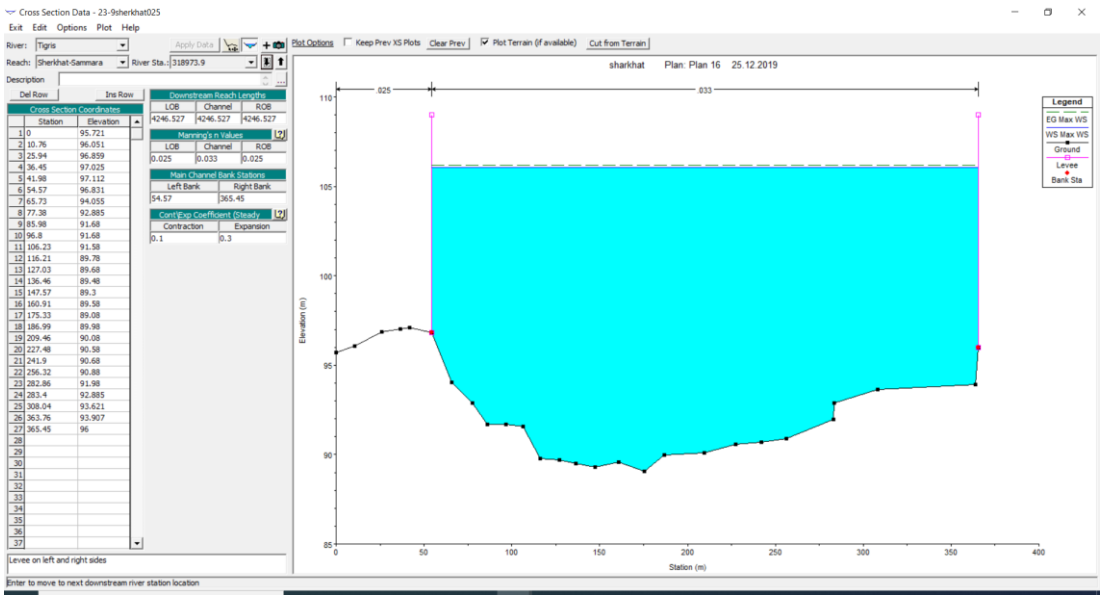

Figure A.6 River cross-section at 18.8 km distance from the upstream

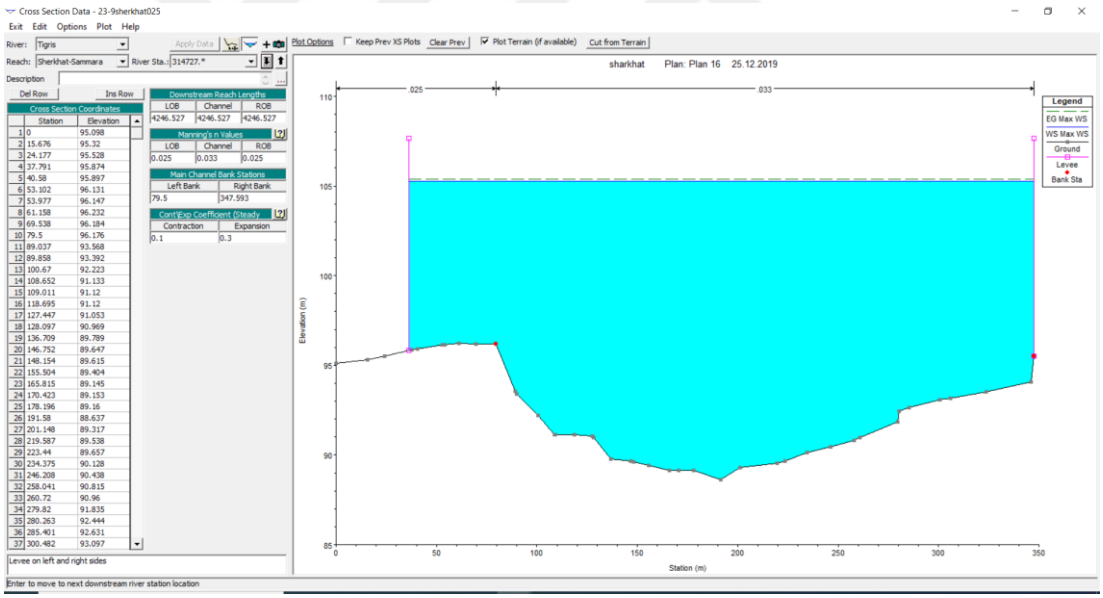

Figure A.7 River cross-section at 23.0 km distance from the upstream

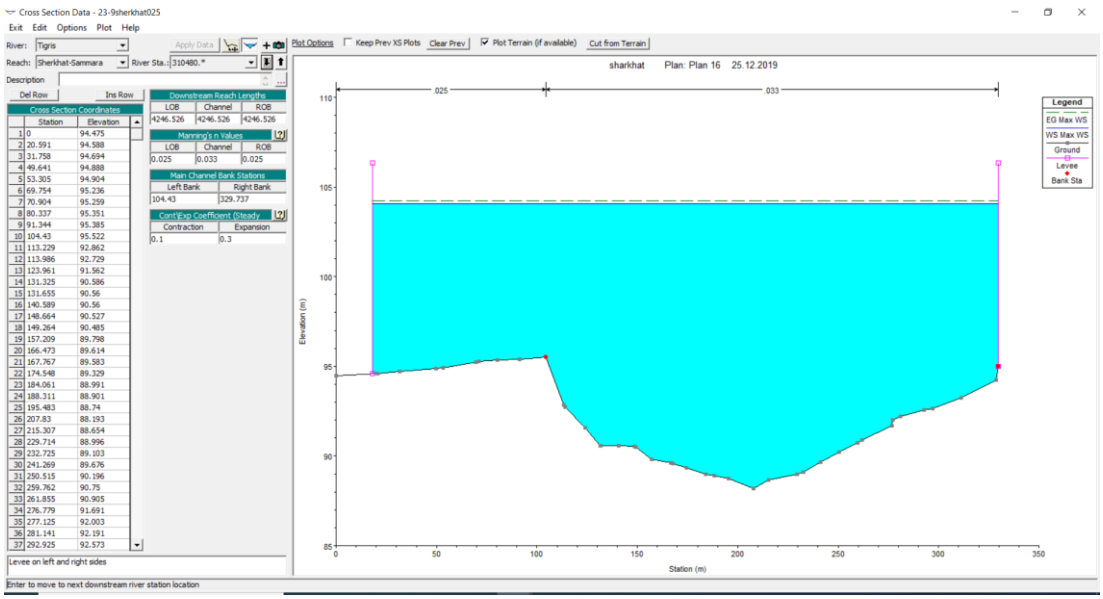

Figure A.8 River cross-section at 27.3 km distance from the upstream

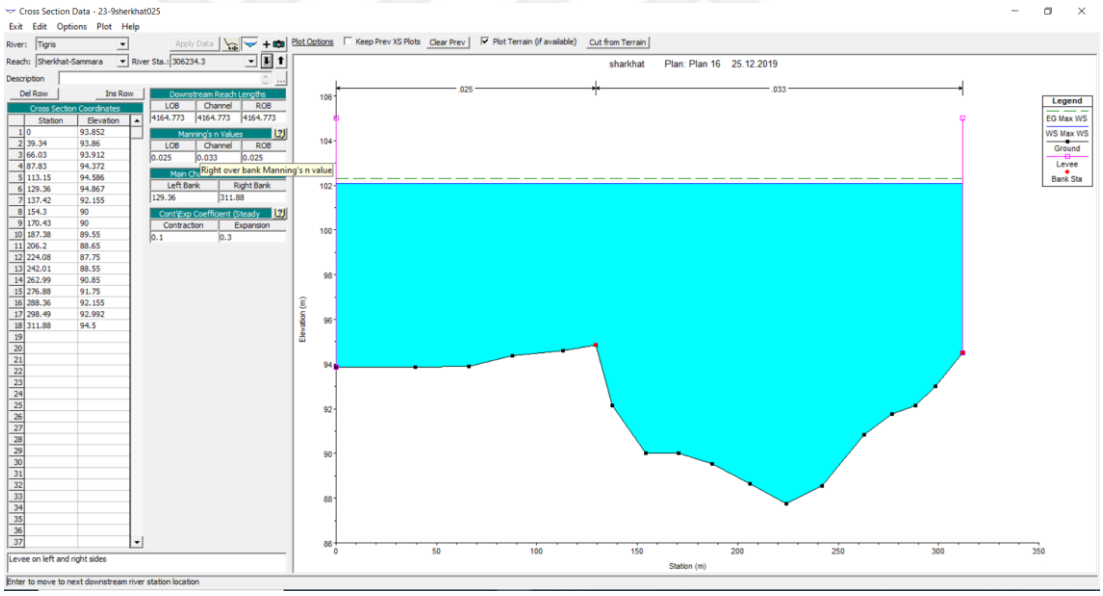

Figure A.9 River cross-section at 31.5 km distance from the upstream

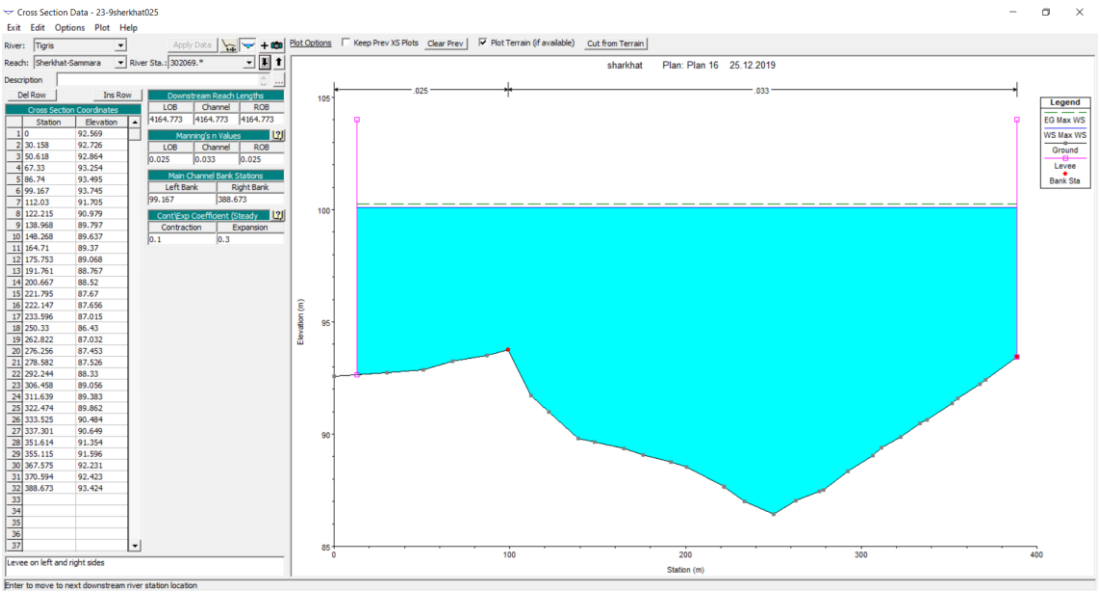

Figure A.10 River cross-section at 35.7 km distance from the upstream

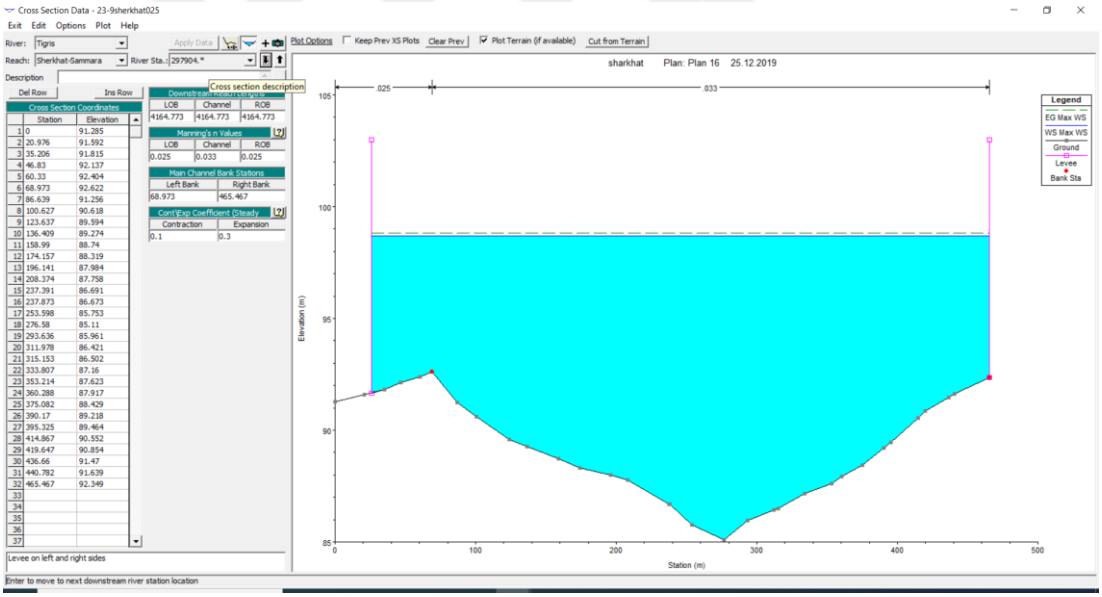

Figure A.11 River cross-section at 39.8 km distance from the upstream

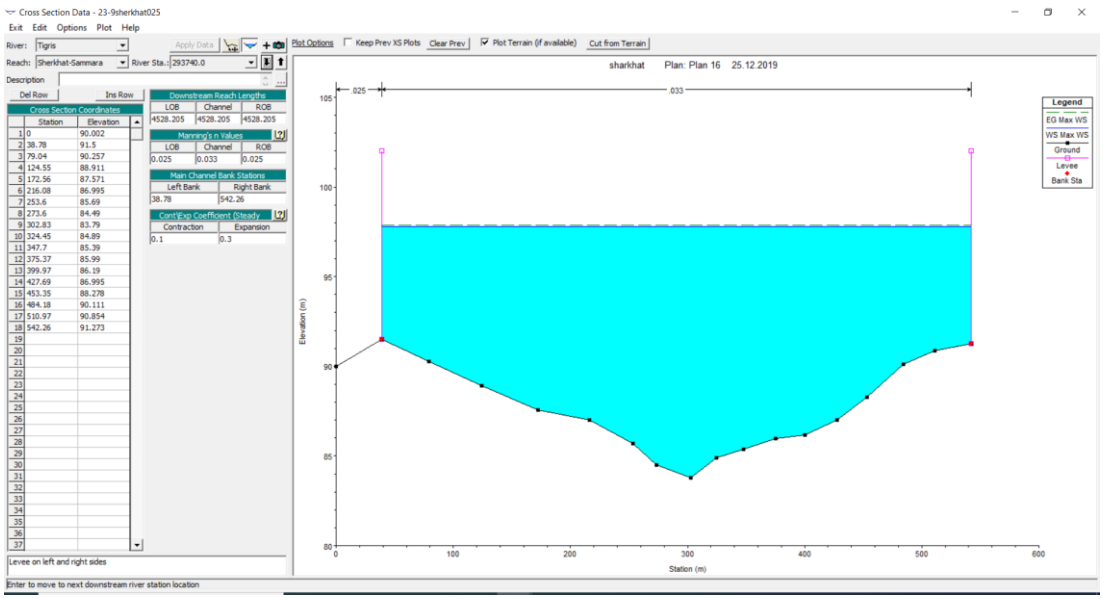

Figure A.12 River cross-section at 44.0 km distance from the upstream

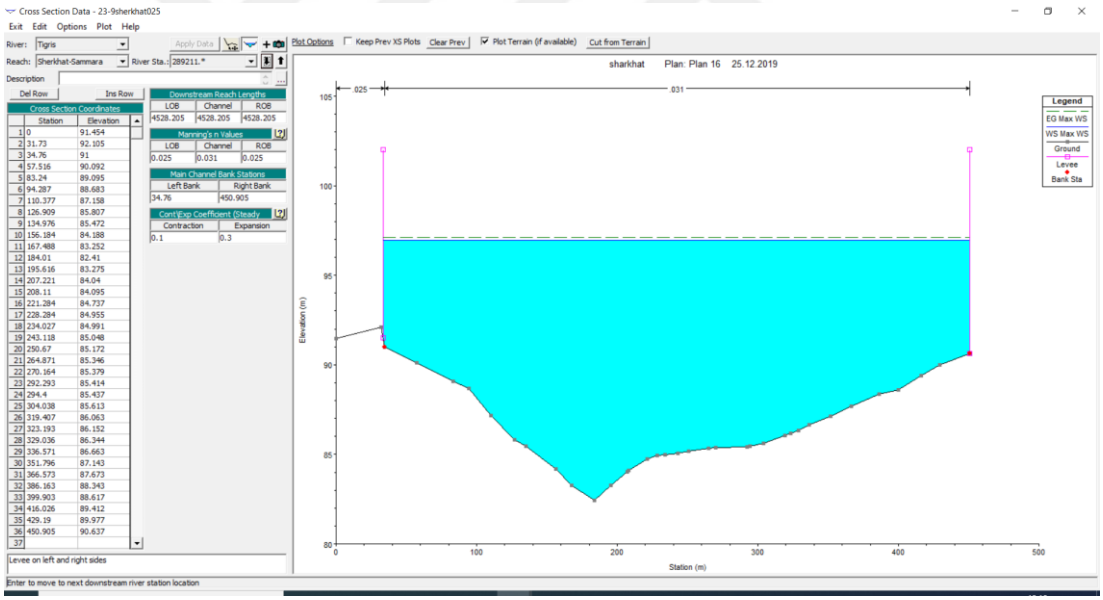

Figure A.13 River cross-section at 48.5 km distance from the upstream

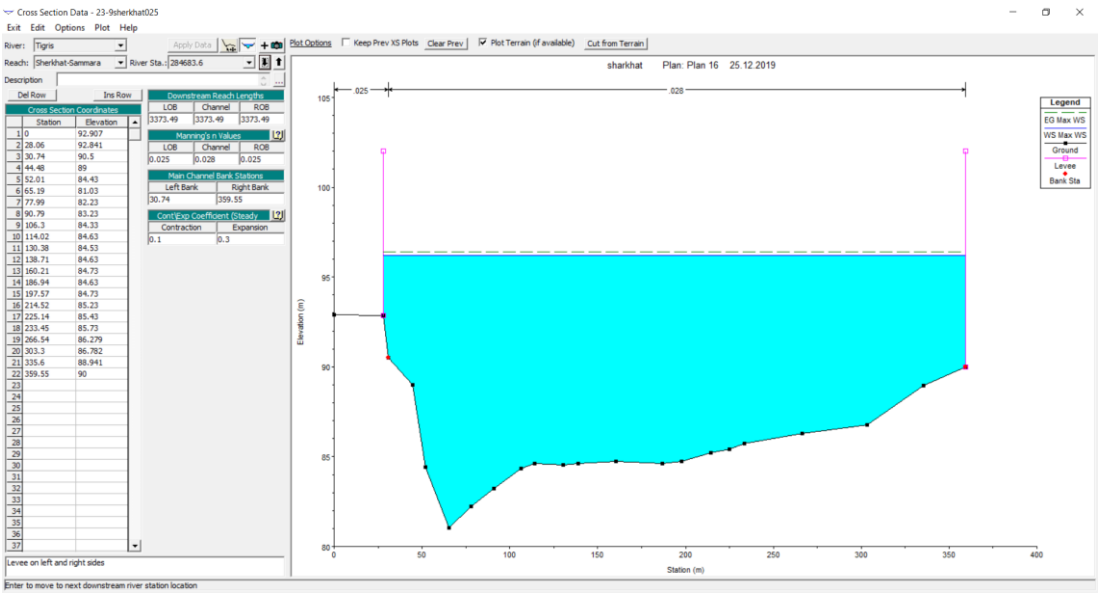

Figure A.14 River cross-section at 53.1 km distance from the upstream

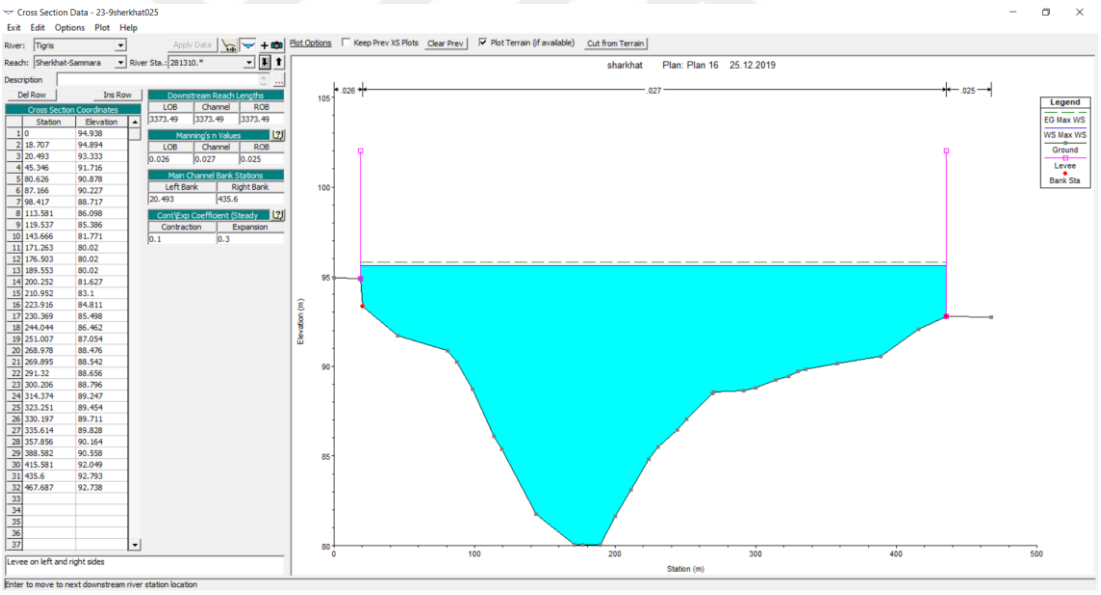

Figure A.15 River cross-section at 56.4 km distance from the upstream

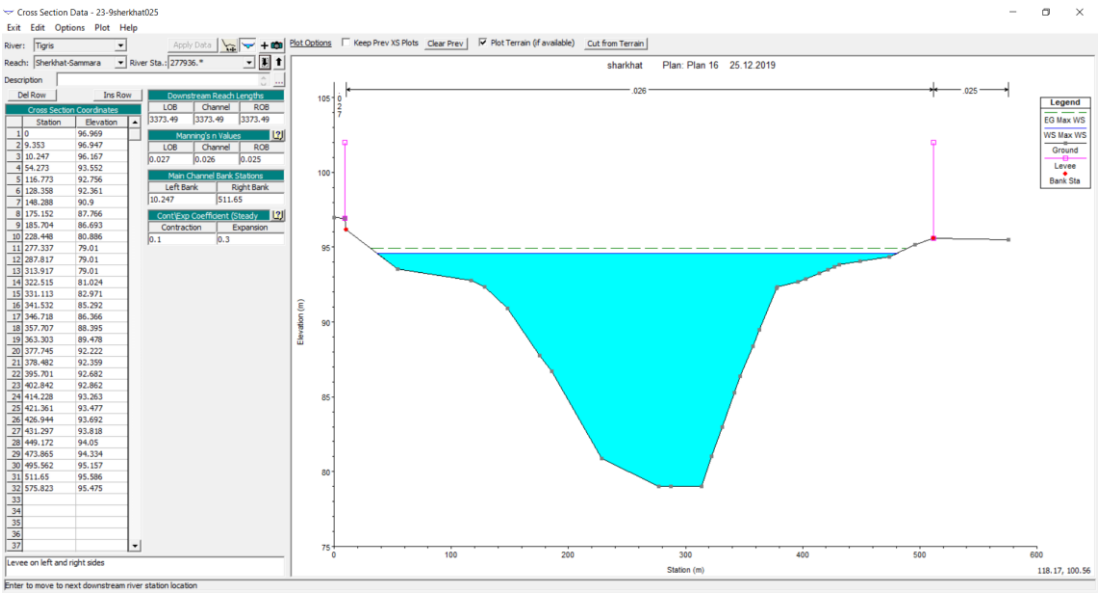

Figure A.16 River cross-section at 59.8 km distance from the upstream

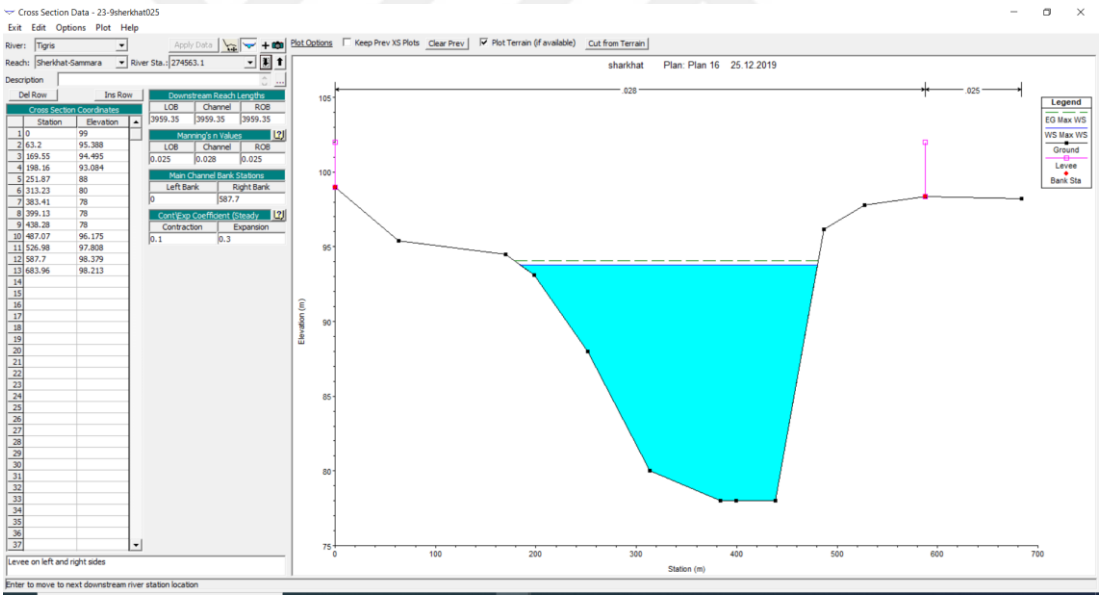

Figure A.17 River cross-section at 63.2 km distance from the upstream

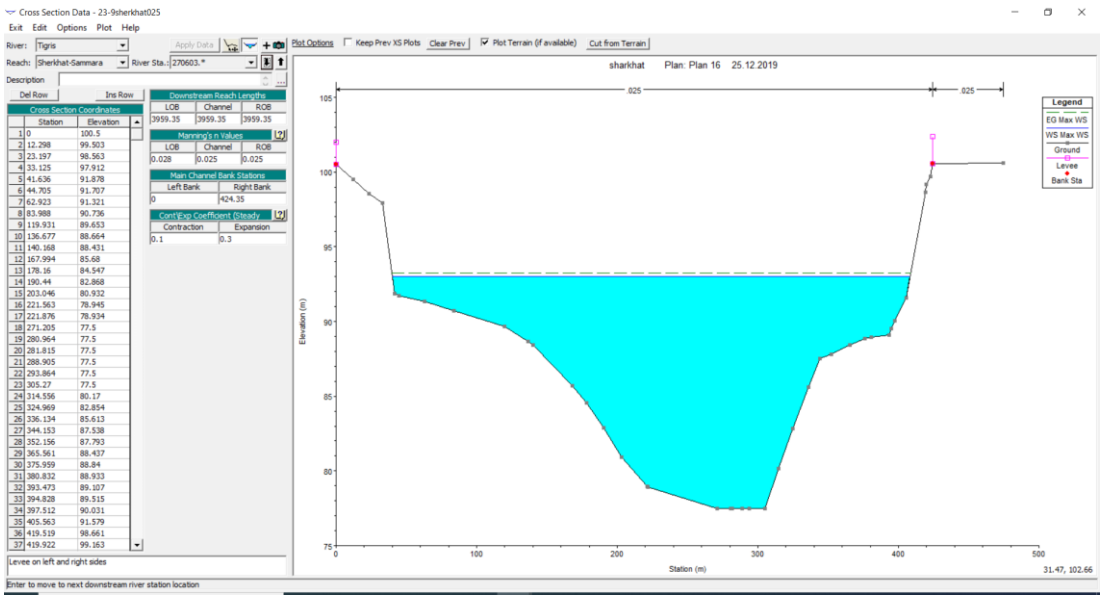

Figure A.18 River cross-section at 67.1 km distance from the upstream

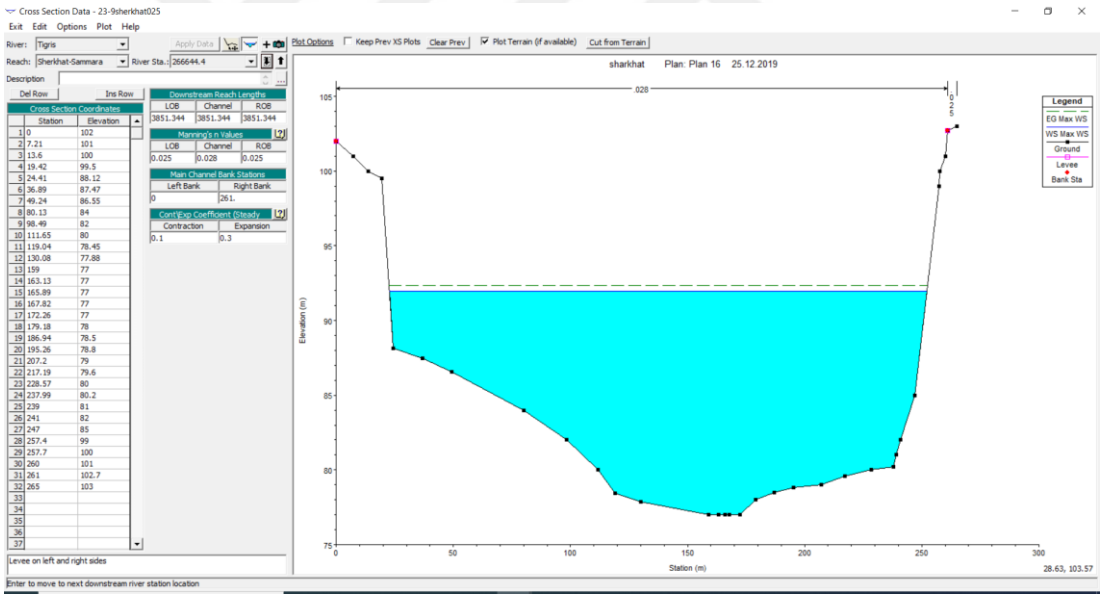

Figure A.19 River cross-section at 71.1 km distance from the upstream

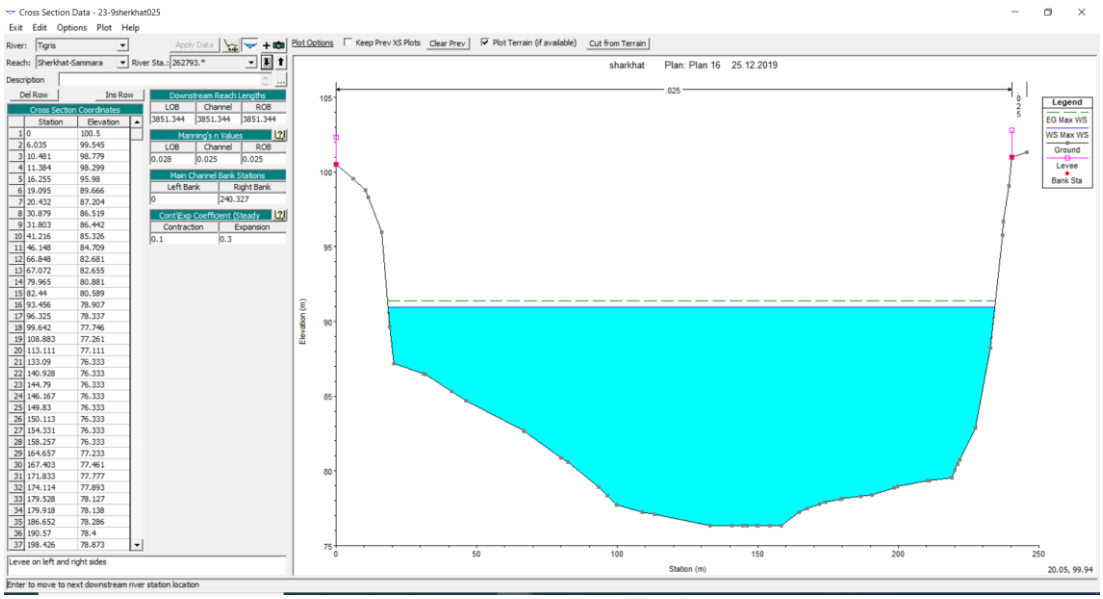

Figure A.20 River cross-section at 74.9 km distance from the upstream

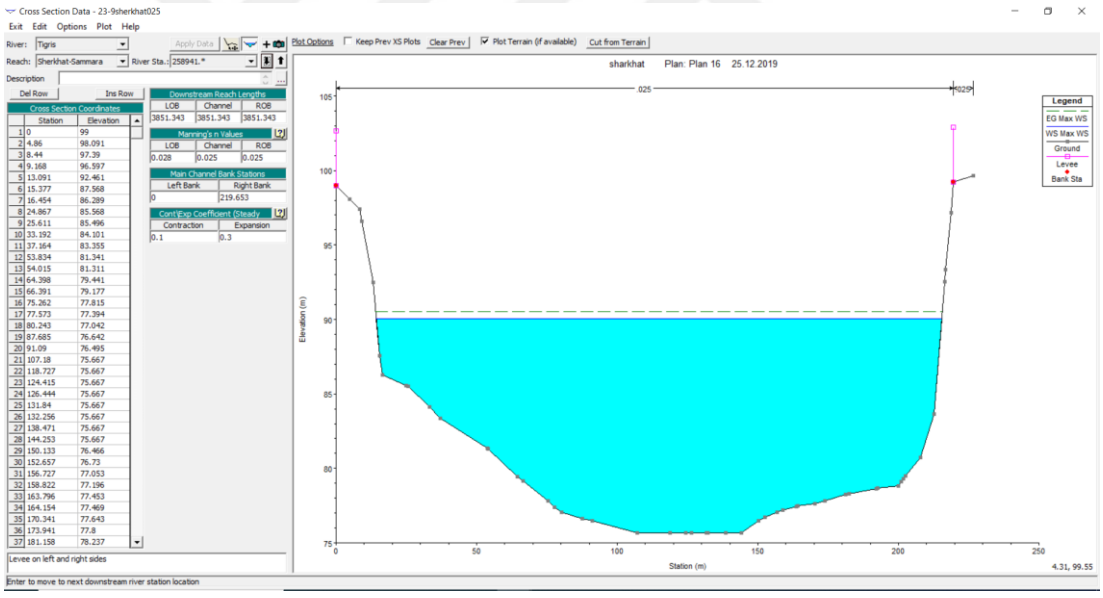

Figure A.21 River cross-section at 78.8 km distance from the upstream

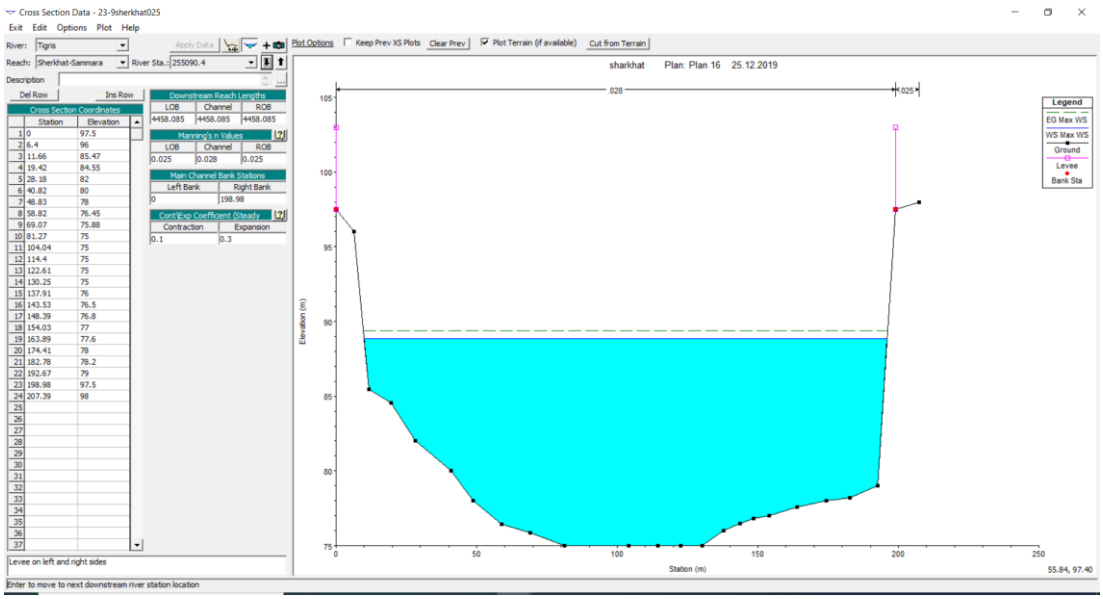

Figure A.22 River cross-section at 82.6 km distance from the upstream

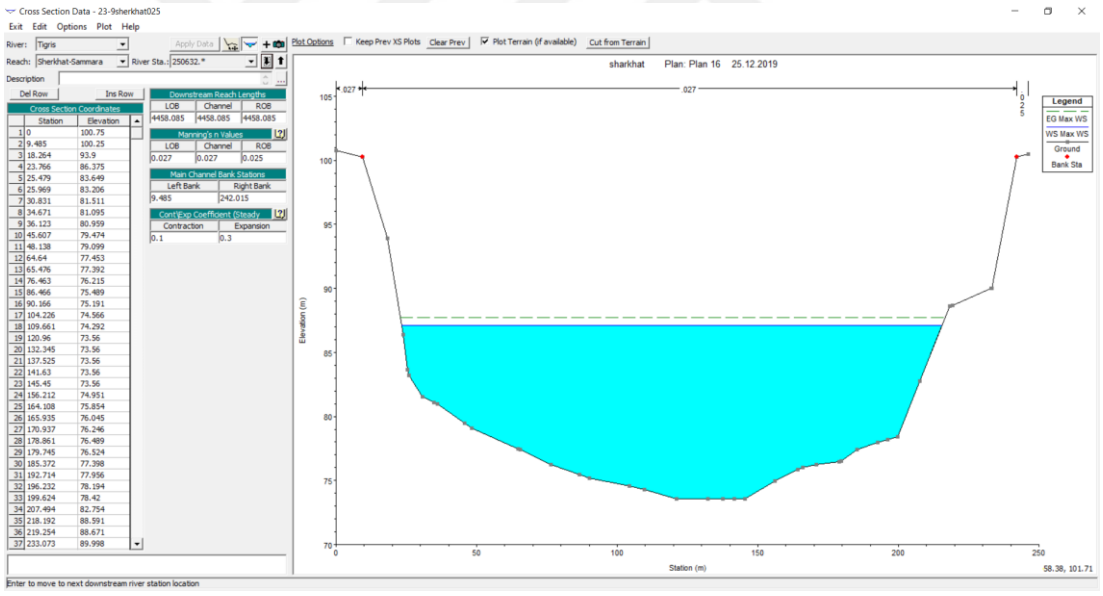

Figure A.23 River cross-section at 87.1 km distance from the upstream

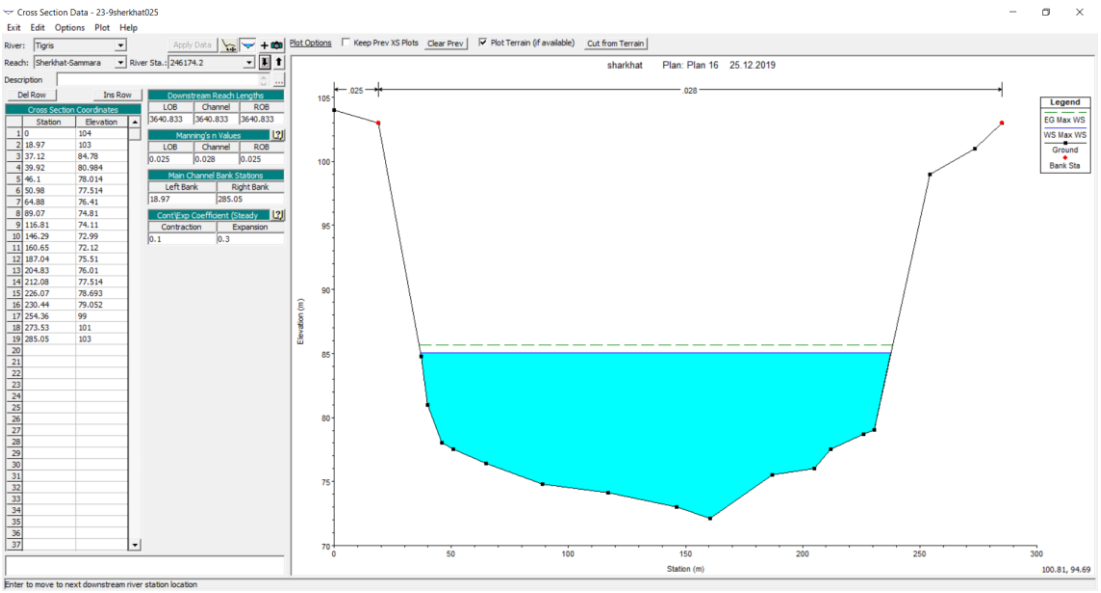

Figure A.24 River cross-section at 91.6 km distance from the upstream

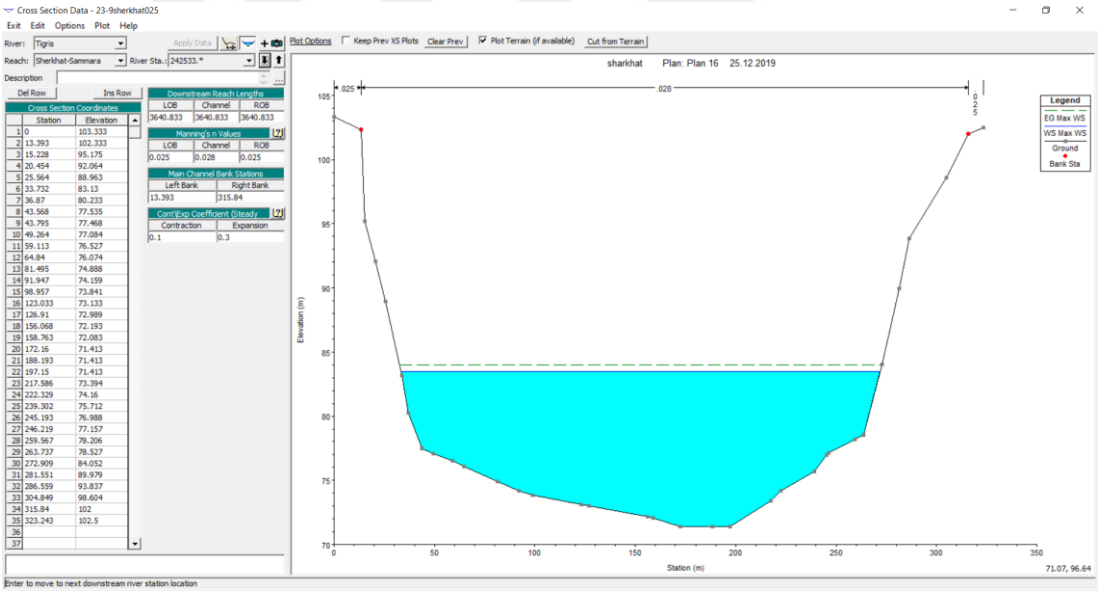

Figure A.25 River cross-section at 95.2 km distance from the upstream

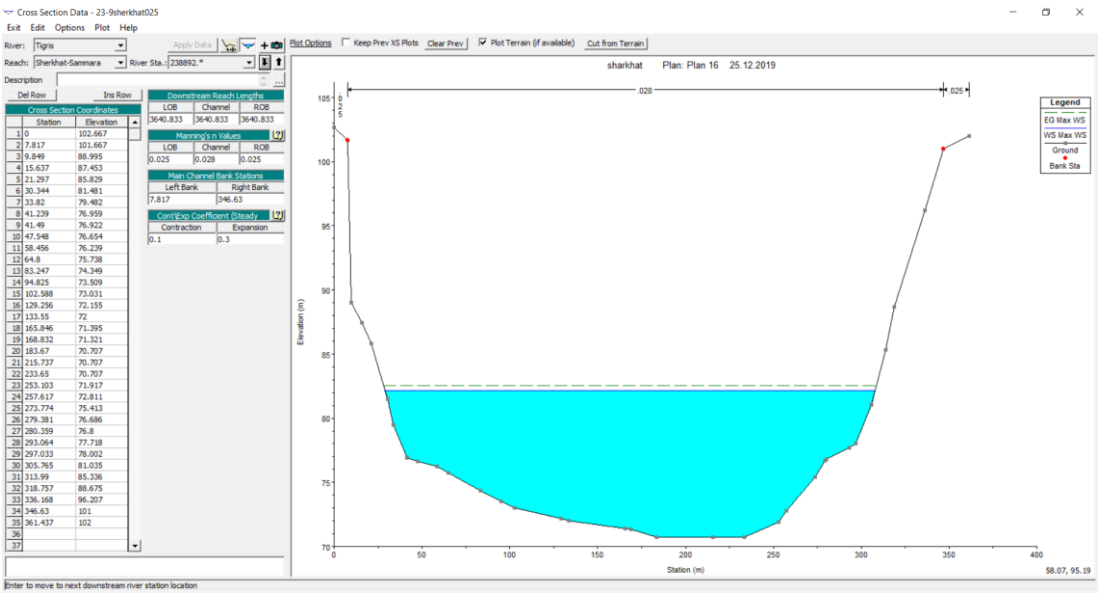

Figure A.26 River cross-section at 98.8 km distance from the upstream

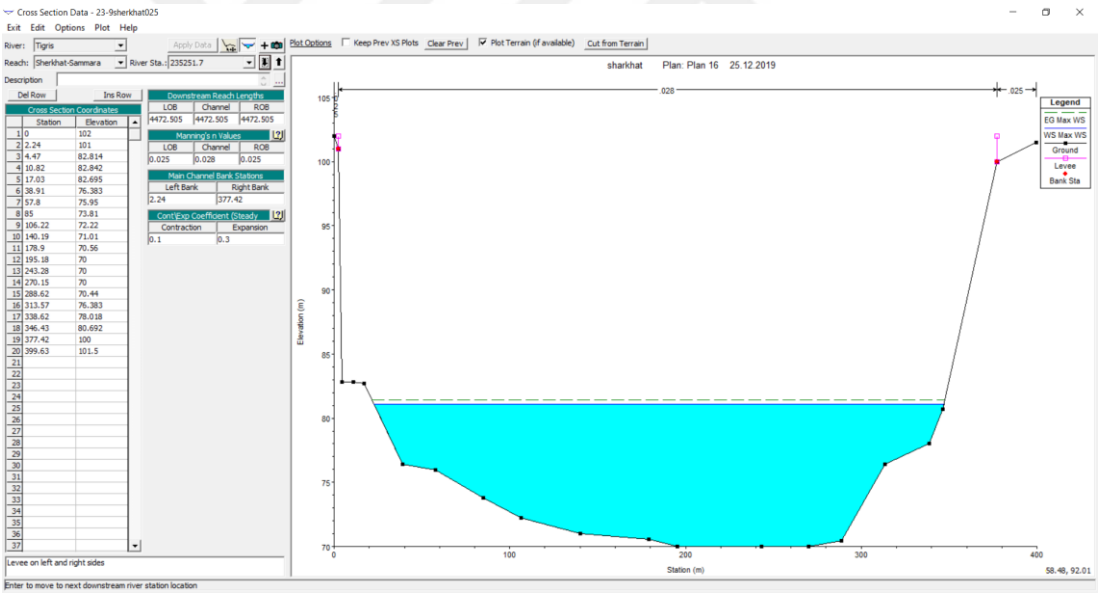

Figure A.27 River cross-section at 102.5 km distance from the upstream

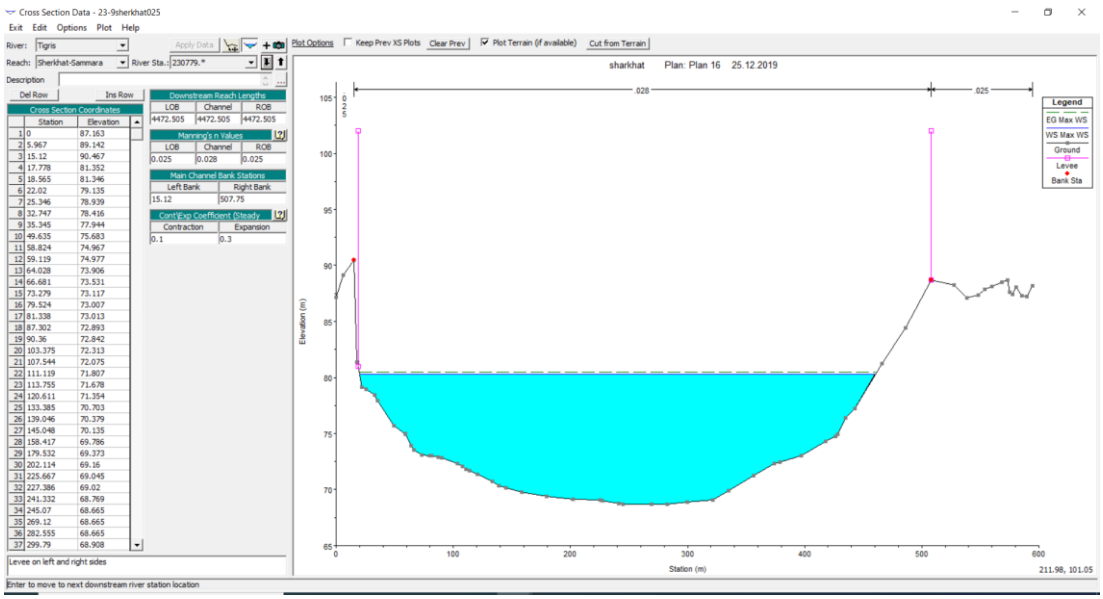

Figure A.28 River cross-section at 107.0 km distance from the upstream

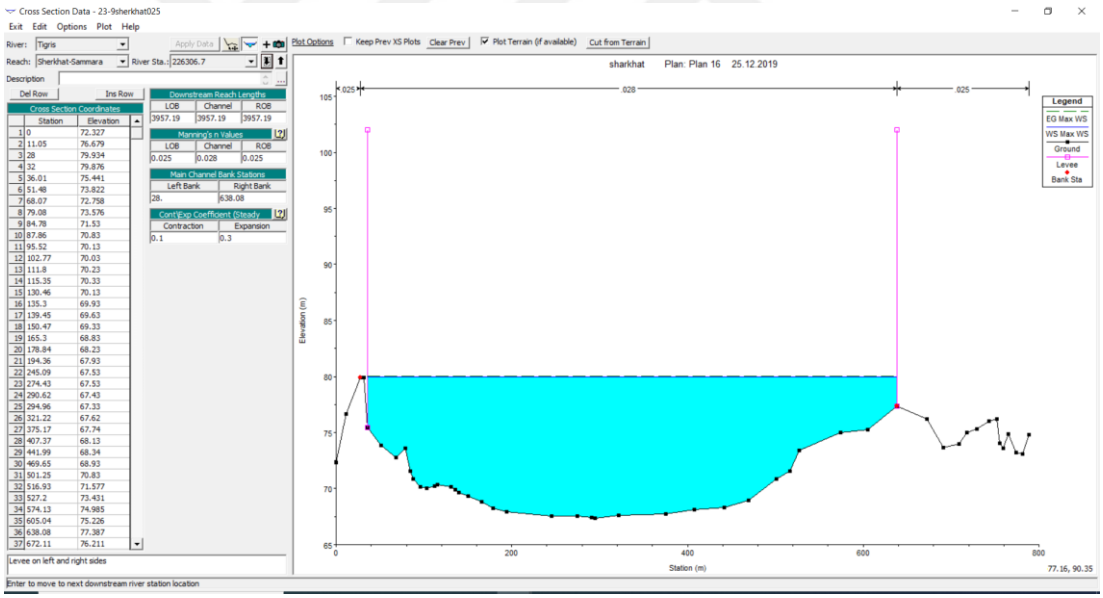

Figure A.29 River cross-section at 111.4 km distance from the upstream

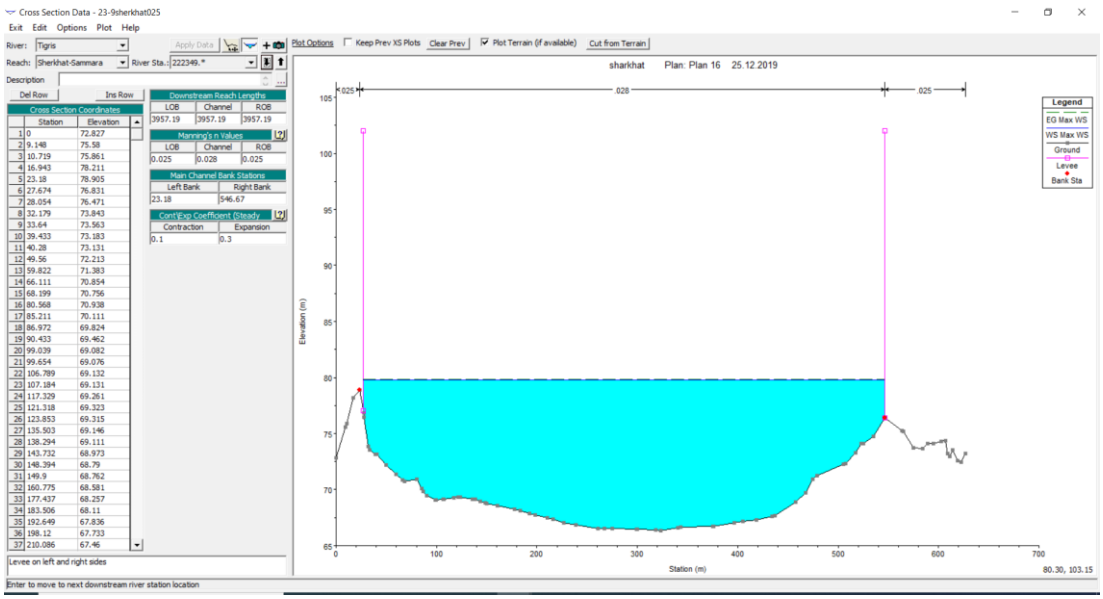

Figure A.30 River cross-section at 115.4 km distance from the upstream

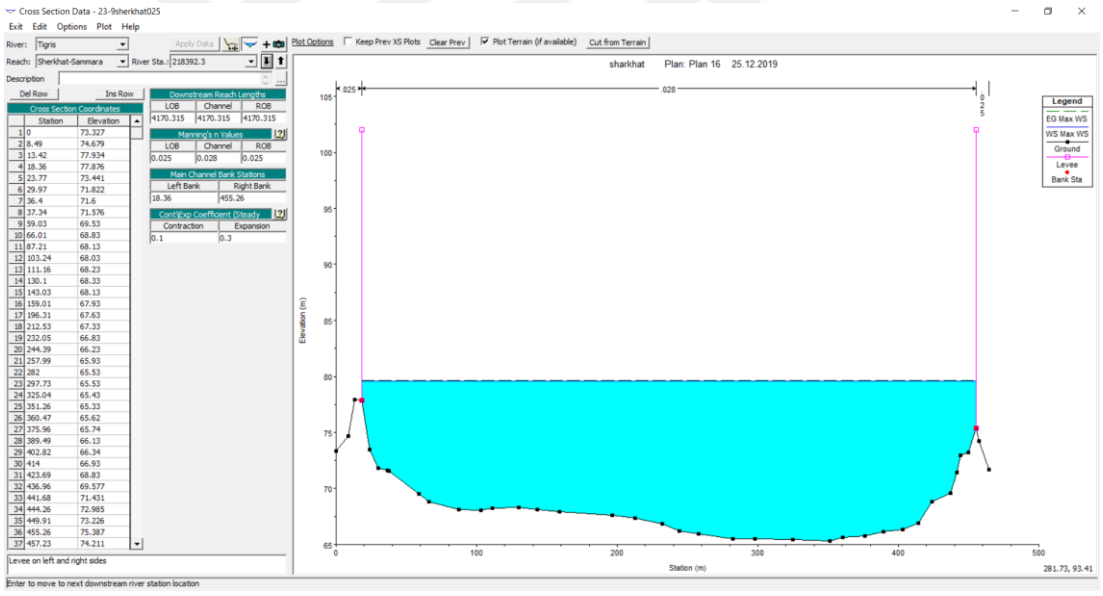

Figure A.31 River cross-section at 119.3 km distance from the upstream

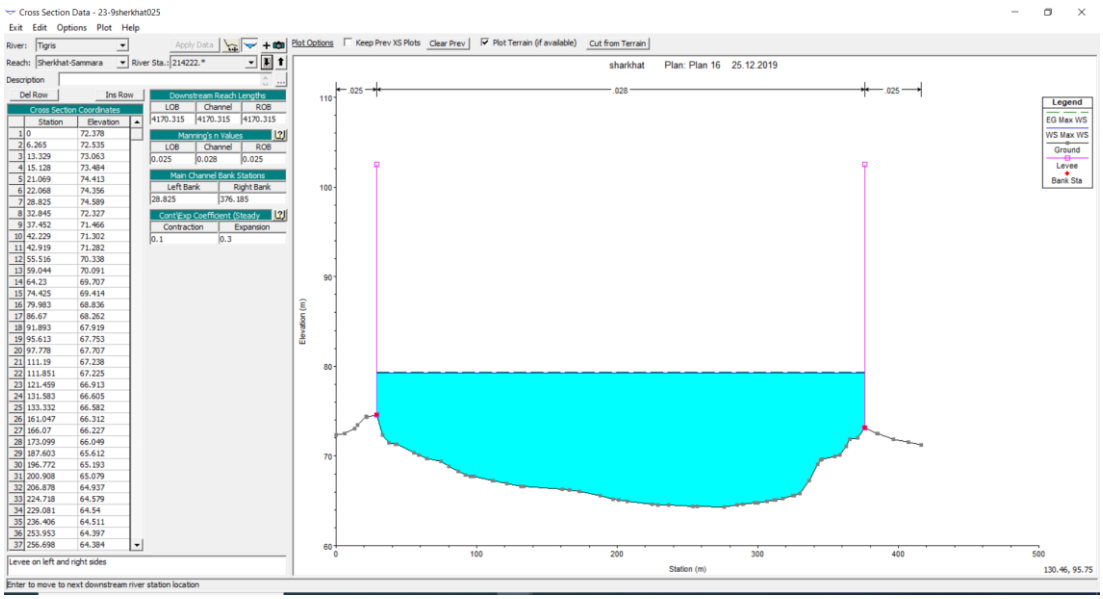

Figure A.32 River cross-section at 123.5 km distance from the upstream

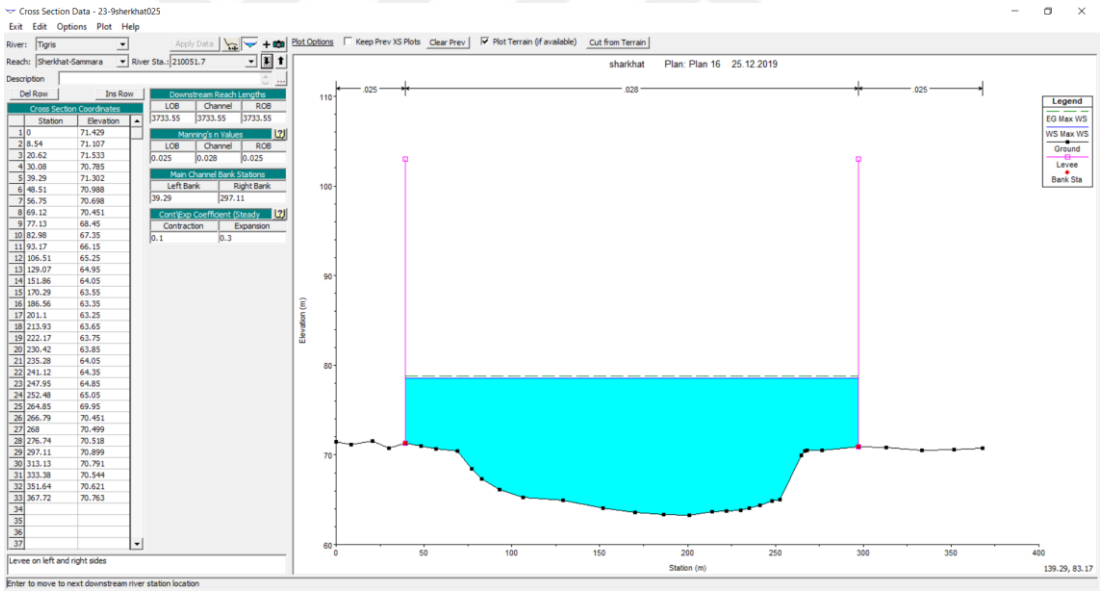

Figure A.33 River cross-section at 127.7 km distance from the upstream

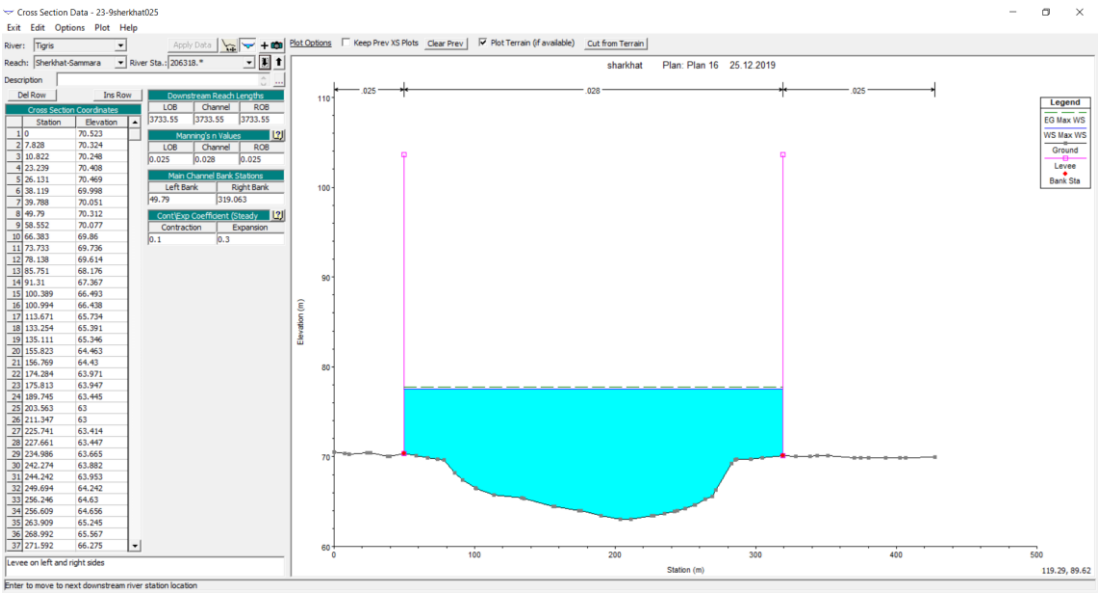

Figure A.34 River cross-section at 131.4 km distance from the upstream

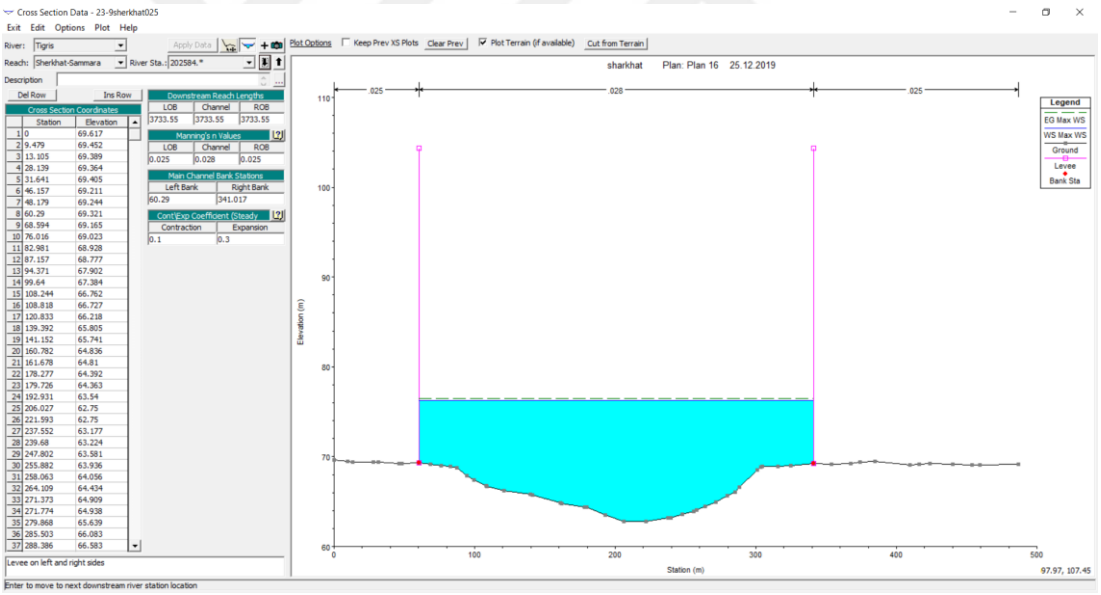

Figure A.35 River cross-section at 135.2 km distance from the upstream

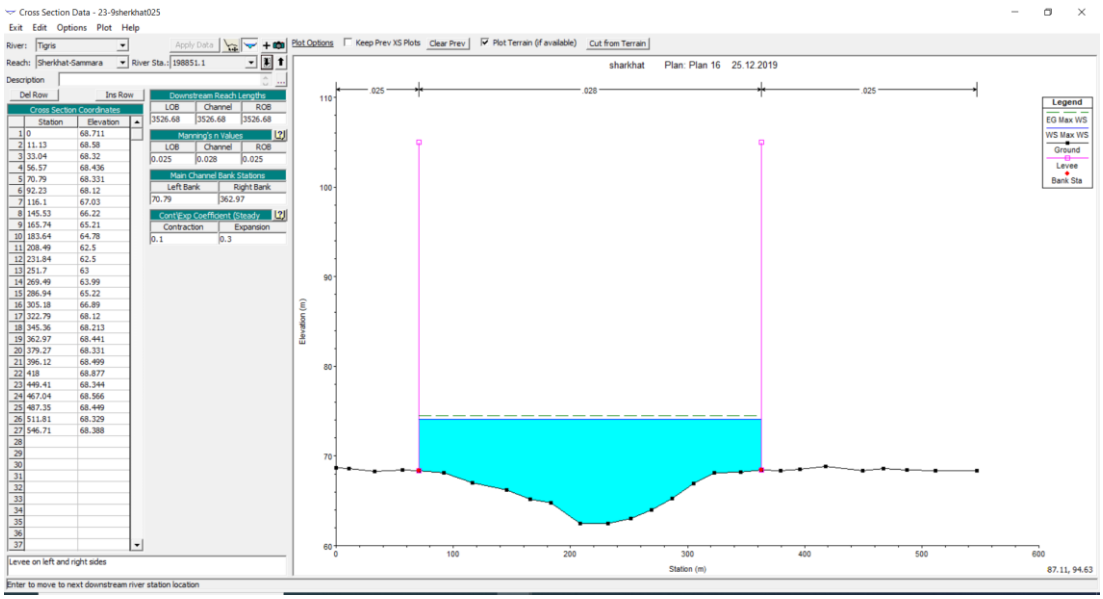

Figure A.36 River cross-section at 138.9 km distance from the upstream

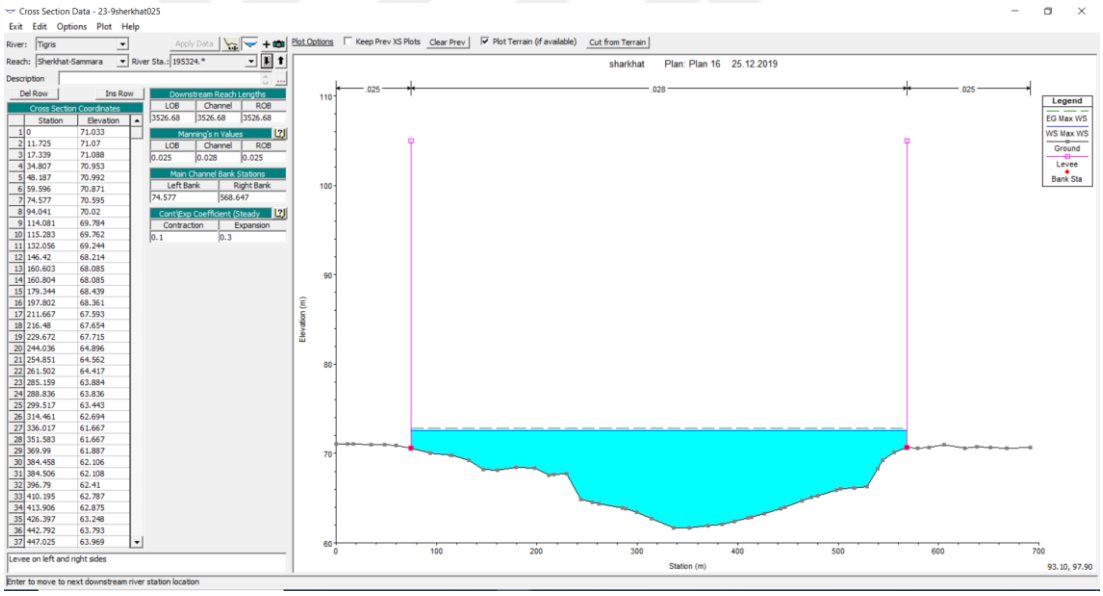

Figure A.37 River cross-section at 142.4 km distance from the upstream

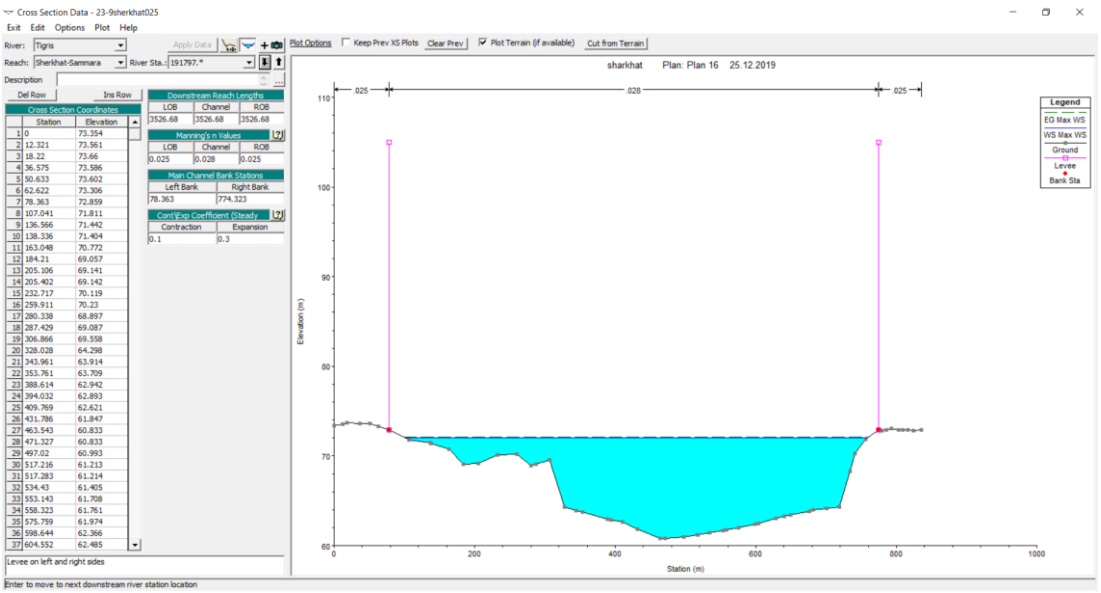

Figure A.38 River cross-section at 145.9 km distance from the upstream

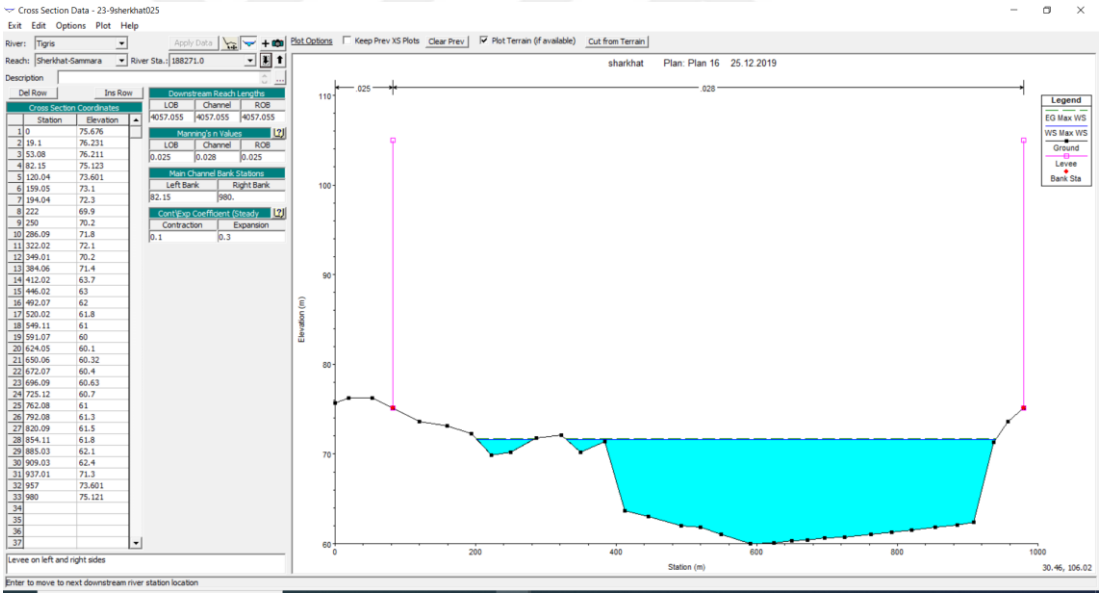

Figure A.39 River cross-section at 149.5 km distance from the upstream

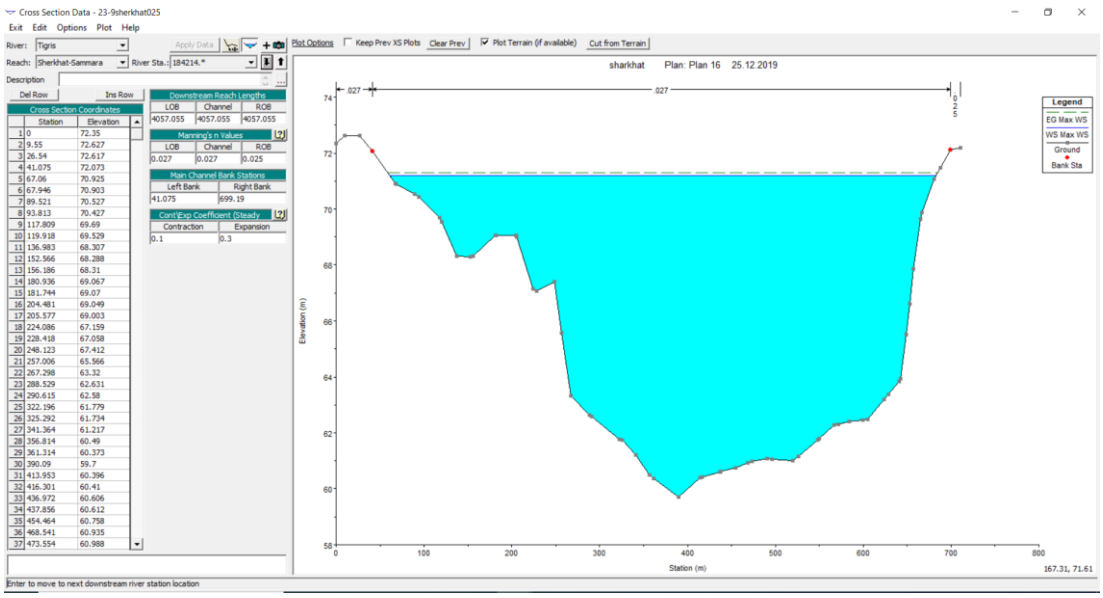

Figure A.40 River cross-section at 153.5 km distance from the upstream

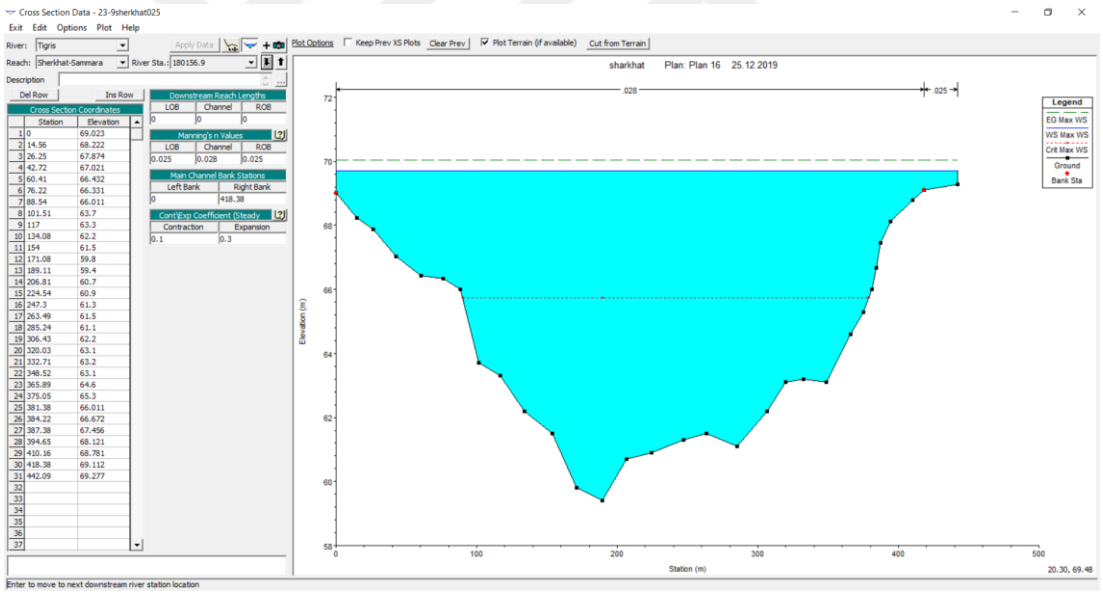

Figure A.41 River cross-section at 157.6 km distance from the upstream